NASA/CR—1998-207938

Nonlinear Interaction of Detuned Instability Waves in Boundary-Layer Transition

Resonant-Triad Interaction

Sang Soo Lee
NYMA, Inc., Brook Park, Ohio

Prepared under Contract NAS3–98022

National Aeronautics and
Space Administration

Lewis Research Center

June 1998

Available from

NASA Center for Aerospace Information
7121 Standard Drive
Hanover, MD 21076
Price Code: A04

National Technical Information Service
5287 Port Royal Road
Springfield, VA 22100
Price Code: A04

NONLINEAR INTERACTION OF DETUNED INSTABILITY WAVES IN BOUNDARY-LAYER TRANSITION: 1. RESONANT-TRIAD INTERACTION

Sang Soo Lee

NYMA, Inc., NASA Lewis Research Center Group, M.S. 5-9

Cleveland, OH 44135

Abstract

The non-equilibrium critical-layer analysis of a system of frequency-detuned resonant-triads is presented using the generalized scaling of Lee (1997a). It is shown that resonant-triads can interact nonlinearly within the common critical layer when their (fundamental) Strouhal numbers are different by a factor whose magnitude is of the order of the growth rate multiplied by the wavenumber of the instability wave. Since the growth rates of the instability modes become larger and the critical layers become thicker as the instability waves propagate downstream, the frequency-detuned resonant-triads that grow independently of each other in the upstream region can interact nonlinearly in the later downstream stage. In the final stage of the non-equilibrium critical-layer evolution, a wide range of instability waves with the scaled frequencies differing by almost $O(1)$ can nonlinearly interact. Low-frequency modes are also generated by the nonlinear interaction between oblique waves in the critical layer. The system of partial differential critical-layer equations along with the jump equations are presented here. The amplitude equations with their numerical solutions are given in Part 2. The nonlinearly generated low-frequency components are also investigated in Part 2.

1. Introduction

Boundary-layer transition usually starts with the spatially growing instability waves as reviewed by Kachanov (1994). When the environmental disturbances are relatively small, the upstream region is dominated by the linear two-dimensional instability waves. The linear two-dimensional behaviour usually persists over long streamwise distances, but the flow eventually becomes three-dimensional. The Λ-shaped structures that have been observed in flow-visualization experiments can either be aligned or staggered in alternating rows. It is believed that the staggered arrangement is the result of a resonant-triad interaction between a pair of subharmonic oblique modes and the fundamental two-dimensional mode (Kachanov 1994). As the flow evolves downstream, the initially small side-band instability modes become large and the peak in the frequency spectrum becomes wider. Eventually, all of the unsteady and steady flow components start to interact nonlinearly and the flow becomes turbulent where it will be governed by the fully elliptic type equations rather than by the equations that are parabolic in the streamwise direction.

A self-consistent theoretical analysis of the nonlinear interaction between frequency-detuned instability waves during the boundary-layer transition process will be presented in this paper. The matched asymptotic method in the high Reynolds number flow will be used as in Goldstein & Lee (1992), who studied the resonant-triad interaction in the adverse-pressure-gradient boundary layer. Since asymptotic analyses of instability waves in high-Reynolds number flows, including critical-layer analyses, are well reviewed by Cowley & Wu (1994), we will only summarize the results of the critical-layer analyses that are closely related to ours.

Goldstein, Durbin & Leib (1987) investigated the nonlinear critical layer in the adverse-pressure-gradient boundary layer for an evolving plane wave. They considered a disturbance that evolves from a linear instability wave similar to the subsequent free shear layer analyses of Goldstein & Leib (1988) and Goldstein & Hultgren (1988). These analyses show that the nonlinear effects first become important in the critical layer. The upstream exponential growth of the linear instability wave is transformed into algebraic growth in the nonlinear region.

It was found by Goldstein & Choi (1989) that a pair of oblique modes in a free shear layer can interact nonlinearly within their common thin critical layer to produce a self-interaction term in the amplitude equation. The self-interaction term causes the oblique waves to grow very fast and ultimately leads to a singularity at a finite downstream position. This oblique mode interaction can occur at much earlier streamwise position, or at smaller amplitudes of the instability waves, than the nonlinear interaction of the plane wave considered by Goldstein *et al.* (1987), Goldstein & Leib (1988) and Goldstein & Hultgren (1988). Goldstein & Choi (1989) also showed that the nonlinear interaction between oblique modes in the critical layer produces a steady mean flow correction term that is periodic in the spanwise direction. The magnitude of this nonlinearly generated component is as big as that of the primary oblique modes outside the critical layer.

In incompressible boundary layer flows, the plane-wave amplitude is usually much larger than the oblique-mode amplitude in the upstream region because the plane wave is the most unstable mode. Thus, the oblique mode interaction of Goldstein & Choi (1989) is not likely to be observed in the early stage of the transition process unless three-dimensional modes are artificially excited. The initial nonlinear interaction will then be a parametric-resonance

interaction as shown in the critical-layer analysis of the resonant-triad by Goldstein & Lee (1992). During the parametric-resonance stage the growth rate of the oblique mode is greatly enhanced. The parametric-resonance interaction produces no velocity jump across the critical layer at the fundamental frequency. That means the two-dimensional wave continues to grow at its initial linear growth rate even when the oblique modes become very large relative to the plane wave. Goldstein & Lee (1992) showed that the oblique modes eventually react back on the plane wave in the fully-coupled stage. The oblique modes also interact nonlinearly between themselves, during this stage, to produce a self-interaction term. This term, which was originally obtained by Goldstein & Choi (1989) in the free shear layer analysis, causes the instability growth to increase beyond the faster-than-exponential growth of the parametric-resonance stage and ultimately leads to a singularity at a finite downstream position. Essentially the same amplitude equations were obtained by Wu (1992) for the resonant-triad interaction in the oscillating Stokes layer.

Wu, Lee & Cowley (1993) included the effect of $O(1)$ viscosity in the critical layer in the oblique mode amplitude equation for the oscillating Stokes layer. Increasing the viscosity generally delays the occurrence of the finite-time singularity. By taking the highly viscous limit of the finite-viscosity amplitude equation, they found that the diffusion layer that surrounds the critical layer must be considered in the viscous quasi-equilibrium critical-layer analysis. The full finite-viscosity amplitude equations including the back-reaction term in the plane-wave amplitude equation were obtained by Wu (1995).

Mankbadi, Wu & Lee (1993) and Wu (1993) showed that, in the Blasius and favorable-pressure-gradient boundary layers, respectively, the dominant nonlinear interactions take place in an intermediate diffusion layer that surrounds the critical layer when the viscous

effect is large. There is no back-reaction effect on the plane wave which therefore continues to grow linearly.

In the non-equilibrium critical-layer analysis by Goldstein & Lee (1992) and Wu (1992), the growth and mean convection (and also viscous) effects can enter the critical-layer dynamics at the same order. However, when the viscous effect becomes large as in Mankbadi *et al.* (1993) and Wu (1993), the mean convection effect balances with the viscous effect inside the critical layer, which we refer to as a (viscous) quasi-equilibrium (or viscous-limit) critical layer.

Wundrow, Hultgren & Goldstein (1994) considered the resonant-triad interaction in the adverse-pressure-gradient boundary layer when the initial amplitude of the oblique mode is small enough so that the plane wave can become strongly nonlinear within its own critical layer (as in Goldstein, Durbin & Leib 1987) before it is affected by the oblique mode. Goldstein (1994, 1995) extended the analysis of Wundrow *et al.* (1994) to the Blasius boundary layer when the initial oblique-mode amplitude is sufficiently small at the start of the parametric resonance. The streamwise evolution of a pair of oblique Tollmien-Schlichting waves in the Blasius boundary layer was studied by Wu, Leib & Goldstein (1997).

The Tollmien-Schlichting waves in the boundary layers are initially governed by quasi-equilibrium critical-layer dynamics as in Mankbadi *et al.* (1993), Wu (1993) and Wu *et al.* (1997). However, the results of the analyses by Goldstein (1994, 1995) and Wu *et al.* (1997) and the numerical solutions of Lee (1997a) (who solved the partial differential critical-layer equations numerically) indicate that the critical layer in the later downstream stage is eventually governed by the non-equilibrium dynamics and the amplitudes of the instability

modes are determined by the inviscid or finite-viscosity amplitude equations (Goldstein & Lee 1992; Wu 1992, 1995; Wu *et al.* 1993) or by the system of critical-layer equations (Lee 1997a) with negligibly small linear growth rates.

Lee (1997a) developed the generalized scaling which can be applied to both the non-equilibrium and quasi-equilibrium critical-layer analyses of zero- and non-zero-pressure-gradient boundary layers. He showed that the scalings in the boundary-layer analyses mentioned above can be recovered by appropriately choosing the parameters introduced in his generalized scaling. The result of the generalized non-equilibrium analysis was presented and the system of partial differential critical-layer equations was solved numerically. Lee (1997a) showed, by extending the analysis of Wu *et al.* (1993), that the quasi-equilibrium amplitude equations of Mankbadi *et al.* (1993) and Wu (1993) can also be derived by taking the viscous limit of the finite-viscosity amplitude equations.

The results of the critical-layer analyses mentioned above show that the later downstream stage of the critical-layer evolution is governed by the non-equilibrium dynamics and the amplitudes of the instability waves become singular at a finite downstream position. The self-interaction between oblique modes is mainly responsible for the explosive growth near the singular point. The thickness of the critical layer becomes very large near the singular point since it is proportional to the magnitude of the growth rate of the instability mode.

However, so far, only a single resonant-triad or a pair of oblique modes of the same frequency has been considered in the previously mentioned studies. In this paper, a system of resonant-triads whose frequencies (of the fundamental waves) are slightly different will be analysed. The frequency-detuned resonant-triads can interact between themselves within the common critical layer when the magnitude of the frequency difference is the same order

as that of the growth rates multiplied by the wavenumbers of the instability waves (Lee 1997b, 1998a).

The growth rates of the instability modes become larger and the critical layers become thicker as the instability waves propagate downstream. The resonant-triads, which initially grow independently of each other since their fundamental frequencies are sufficiently detuned, start to interact nonlinearly in the downstream position where their growth rates become large enough to be equal to the magnitude of the phase speed difference (or the frequency difference divided by the wavenumber). This implies that most of the unstable waves whose scaled frequency differences are nearly $O(1)$ can interact between themselves right before the triple-deck stage where the magnitude of the growth rates and that of the wavenumbers are the same. The flow in the triple-deck stage will be governed by the unsteady, inviscid, three-dimensional triple-deck equations (Goldstein & Lee 1992, 1993; Wu *et al.* 1997).

The overall plan of the paper is as follows. The problem is formulated and the generalized scaling is presented in §2. The non-equilibrium critical-layer analysis is given in §3 to §7. The solutions in the main boundary layer are given in §3 and those in the viscous Stokes layer are presented in §4. In §5 we show that the linear Tollmien solution in the inviscid wall layer can be matched onto the solutions of the main boundary layer and of the viscous Stokes layer. The derivations of the critical-layer equations and the jump conditions are explained in §6. The system of partial differential critical-layer equations and the jump equations with appropriate upstream matching conditions are presented in §7. The amplitude equations which are obtained by solving the system of critical-layer equations in §7 analytically will be presented in Part 2 (Lee 1998b) together with their numerical solutions.

The low-frequency spanwise-periodic components that are generated by the oblique-mode interaction in the critical layer will be investigated in Part 2.

2. Formulation and scaling

The streamwise, transverse and spanwise coordinates x, y and z are normalized by the local boundary-layer thickness Δ. The mean flow velocity U and the total flow velocity $\mathbf{u} = \{u, v, w\}$ are normalized by the local free-stream velocity U_∞. The pressure p is normalized by ρU_∞^2 and the time t is normalized by Δ/U_∞. We suppose that the mean boundary-layer flow is nearly two-dimensional and the local Reynolds number $R_\Delta (= U_\infty \Delta/\nu)$ is sufficiently large, so that the unsteady flow is nearly unaffected by boundary-layer growth over the region where nonlinear interaction occurs. The base mean flow is nearly parallel and develops slowly on the long viscous scale,

$$x_v = x/R_\Delta. \tag{2.1}$$

The normalized complex wavenumber α of an unstable mode is small and its imaginary part is much smaller than its real part (Drazin & Reid 1981; Smith & Bodonyi 1982; Goldstein *et al.* 1987).

Following the generalized critical-layer scaling of Lee (1997a), we introduce the wavenumber parameter σ and the growth-rate parameter σ^r to characterize the small wavenumber and the ratio of the small growth rate to the wavenumber, respectively. We are interested in the nonlinear interaction of a system of instability waves which is composed of $2J + 1$ resonant-triads (Lee 1997b, 1998a). The jth resonant triad is composed of a single two-dimensional mode of frequency ω_j and wavenumber α_j, and a pair of subharmonic

oblique modes of frequency $\omega_j/2$, streamwise wavenumber nearly equal to $\alpha_j/2$ and spanwise wavenumbers $\pm\beta_j$, where the subscript j can vary from $-J$ to J. The phase speed of the plane wave is assumed to be equal to that of the oblique modes of the same resonant-triad to the required level of approximation, which is the phase-speed resonance condition for the single-resonant-triad interaction. This resonance condition is satisfied when the propagation angle of the oblique mode, defined by (5.29), is about $\pi/3$. It is assumed, in addition, for the multi-resonant-triad interaction that the phase speeds (of the plane waves) of the resonant-triads are nearly equal to one another.

The non-equilibrium critical-layer analysis of a system of resonant-triads will be obtained with the generalized scaling of Lee (1997a). The mean convection effect balances with the growth and viscous (in the finite-viscosity case) effects in the non-equilibrium critical layer (Goldstein & Lee 1992). The recent studies by Goldstein (1994, 1996), Wu *et al.* (1997) and Lee (1997a) indicate that the later nonlinear critical-layer stage is governed by the non-equilibrium dynamics of Goldstein & Lee (1992) even though the earlier stage is governed by the quasi-equilibrium dynamics of Mankbadi *et al.* (1993) and Wu (1993). We only present the details of the non-equilibrium critical-layer analysis since the nonlinear interactions between frequency-detuned instability waves are important in the later stages of the streamwise evolution of instability modes. However, as will be given in Part 2, we can easily obtain the frequency-detuned quasi-equilibrium amplitude equations by taking the viscous limit (Wu *et al.* 1993) of the finite-viscosity amplitude equations as shown by Lee (1997a) for the single-resonant-triad case.

The generalized scaling of Lee (1997a) can be written for the non-equilibrium critical-

layer analysis as

$$\alpha_j = \sigma[\bar{\alpha}_j + O(\sigma^r)], \quad \ddot{c}_j = \sigma[\bar{c}_j + O(\sigma^r)], \quad c_j = \sigma[\bar{c}_j + O(\sigma^r)], \quad \beta_j = \sigma\bar{\beta}_j, \quad y_{cj} = \sigma Y_{cj}, \tag{2.2}$$

$$x_1 = \sigma^{r+1}x, \tag{2.3}$$

$$\mu = \sigma^{r-1}\bar{\mu} \quad \text{for} \quad 1 \leqslant r \leqslant 3 \quad \text{and} \quad \mu = O(1) \quad \text{for} \quad 0 < r \leqslant 1, \tag{2.4}$$

where σ characterizes the small wavenumber as mentioned before, $\ddot{c}_j$ and c_j are the (nearly equal) phase velocities of the two-dimensional and oblique modes respectively, β_j represents the spanwise wavenumber of the oblique modes, y_{cj} is the critical level where the base mean-flow velocity is equal to the real part of the phase velocity, $\bar{\alpha}_j$, $\bar{c}_j$, $\bar{\beta}_j$ and Y_{cj} are order-one real constants (which depend on σ) and $\mu(\equiv R_\Delta dP/dx)$ is the normalized mean pressure gradient. The subscript j is used to denote the quantities of the jth resonant triad. The real part of $\ddot{c}_j$ is only different from that of c_j by $O(\sigma^{r+1})$ as required by the phase-speed resonance condition for the single-resonant-triad interaction. When r is equal to 3 and $\bar{\mu}$ is an order-one real positive constant, $\sigma^{r-1}\bar{\mu} \ll 1$ characterizes the small adverse pressure gradient as in Goldstein & Lee (1992). However, we now allow $\bar{\mu}$ to be non-positive in order to extend the scaling to the Blasius and favorable-pressure-gradient boundary layers. The magnitude of $\bar{\mu}$ could be smaller than $O(1)$ in many important cases, i.e. in the later downstream stages of the nonlinear evolution of instability waves in boundary layers (Wundrow *et al.* 1994; Goldstein 1994, 1996; Wu *et al.* 1997; Lee 1997a).

The scaled Strouhal number $\bar{s}_j$, which is a real constant, of the fundamental two-dimensional mode of the jth resonant-triad is given by

$$s_j = \sigma^2\bar{s}_j = \sigma^2\bar{\alpha}_j\bar{c}_j, \tag{2.5}$$

where the frequency or unscaled Strouhal number s_j of the plane wave is equal to $\alpha_j \ddot{c}_j$ (see (3.7)). We are interested in the case when the scaled Strouhal number of the jth resonant-triad is different from that of the 'reference' 0th resonant-triad by a small factor whose magnitude is of the order of the growth-rate parameter σ^r,

$$\bar{s}_j = \bar{s}_0(1 + \sigma^r j\chi) \quad \text{for} \quad -J \leqslant j \leqslant J, \tag{2.6}$$

where the frequency-detuning factor χ is an order-one real constant. It will be shown by (5.22) that the scaled phase velocities $\bar{c}_j$ for $j = -J, \ldots, J$ are different one another by $O(\sigma^r)$, therefore, the additional resonance condition for the multi-resonant-triad interaction is satisfied.

If the Strouhal number s_j and the small parameter σ are chosen (these parameters can be chosen from experiments and appropriate scalings for the specific problem), the wavenumber $\bar{\alpha}_j$ can be determined from the long-wavelength small-growth-rate dispersion relations (5.8) – (5.13) in §5. The phase speed $\bar{c}_j$ can be obtained from (2.5) and then the critical level y_{cj} which is defined as the transverse location where

$$U\,(y = y_{cj}) = \sigma \bar{c}_j, \tag{2.7}$$

is determined if the base mean flow U is known.

The non-equilibrium critical-layer analysis by Goldstein & Lee (1992) shows that the nonlinear interaction between instability waves of a resonant-triad first occurs within the critical layer whose thickness is of the order of σ^{r+1}. When $\bar{s}_j$ is given by (2.6) the critical level of the jth resonant-triad, y_{cj} is only different from that of the 0th resonant-triad, y_{c0} by $O(\sigma^{r+1})$ (see (5.22)). Therefore, all of the instability waves of the detuned resonant-triads will then nonlinearly interact between themselves within the overlapped critical layers.

The viscous effects will enter the critical-layer momentum equation while making only relatively insignificant modifications to the external flow when the viscous parameter (Benney & Bergeron 1969; Haberman 1972)

$$\lambda \equiv 1/(\sigma^{3r+4} R_\Delta) \tag{2.8}$$

is order one. The scalings for the amplitudes are, following the previous studies by Goldstein & Lee (1992, 1993) and Lee (1997a), for all j,

$$\epsilon_{2d} = \sigma^{4r+1}, \quad \delta_{3d} = \delta_{02} = \sigma^{3r+1}, \tag{2.9}$$

where ϵ_{2d} and δ_{3d} are the amplitude scalings of the two-dimensional and oblique waves. The nonlinear interaction between oblique modes in the critical layer produces a term which is periodic in the spanwise direction (Goldstein & Choi 1989). This term is large in the sense that its magnitude δ_{02} is equal to δ_{3d}. This nonlinearly generated term becomes a function of a slow time, as will be shown in (5.30), in the multi-frequency and multi-resonant-triad cases considered in this study, though it is independent of time in the single-frequency (Goldstein & Choi 1989) or single-resonant-triad (Goldstein & Lee 1992) cases.

The nonlinear interactions between instability waves occur within the critical layer whose thickness is of the same order of magnitude as the growth rate, i.e. $O(\sigma^{r+1})$. We do not need to include the diffusion layer (c.f. Mankbadi *et al.* 1993; Wu 1993) since it is inseparable from the critical layer in the non-equilibrium critical-layer scaling (Lee 1997a). The viscous Stokes layer does not make a leading-order contribution to the growth rate in the non-equilibrium analysis. However, in order to make the analysis valid in the viscous limit we will include the effect of the viscous Stokes layer whose thickness is of the order of $\sigma^{3r/2+1}$. A schematic diagram of the multi-layer structure is given in figure 1 with the

critical levels of the 0th, Jth and $-J$th resonant-triads indicated. The distance from the wall to the jth critical level is y_{cj} that is of $O(\sigma)$ (see (5.22) for their relative positions).

Finally, we will assume that $0 < r \leqslant 3$ for the simplicity. This range of r covers most of the important types of boundary-layer flows as was summarized in table 1 of Lee (1997a).

3. Main boundary layer

Since the unsteady flow outside the critical layer is mostly governed by linear dynamics to the required order of approximation, the velocity field of a system of $2J+1$ resonant-triads in the main boundary layer, where y is of order one, can be written as

$$u = U(y, x_v) + \epsilon_{2d} \sum_{j=-J}^{J} \mathrm{Re}\, \tilde{B}_j \ddot{\Phi}_{jy} e^{\mathrm{i}X_j} + \delta_{3d} \sum_{j=-J}^{J} \mathrm{Re}\, 2\tilde{A}_j \tilde{U}_j(y, x_1) e^{\mathrm{i}X_j/2} \cos Z_j + \delta_{02} \sum_{j} \sum_{\ell} \mathrm{Re}\, \tilde{U}_{0,2;j,\ell}(y, x_1, z, t) + \ldots, \tag{3.1}$$

$$v = V(y, x_v) - \epsilon_{2d} \sum_{j=-J}^{J} \mathrm{Re}\, \mathrm{i}\alpha_j \tilde{B}_j(x_1) \ddot{\Phi}_j(y, x_1) e^{\mathrm{i}X_j} - \delta_{3d} \sum_{j=-J}^{J} \mathrm{Re}\, 2\mathrm{i}\gamma_j \tilde{A}_j(x_1) \Phi_j(y, x_1) e^{\mathrm{i}X_j/2} \cos Z_j + \ldots, \tag{3.2}$$

$$w = \delta_{3d} \sum_{j=-J}^{J} \mathrm{Re}\, 2\mathrm{i}\tilde{A}_j \tilde{W}_j(y, x_1) e^{\mathrm{i}X_j/2} \sin Z_j + \ldots, \tag{3.3}$$

$$p = P + \epsilon_{2d} \sum_{j=-J}^{J} \mathrm{Re}\, \tilde{B}_j \bar{P}_j(y, x_1) e^{\mathrm{i}X_j} + \delta_{3d} \sum_{j=-J}^{J} \mathrm{Re}\, 2\tilde{A}_j \tilde{P}_j(y, x_1) e^{\mathrm{i}X_j/2} \cos Z_j + \ldots, \tag{3.4}$$

with

$$X_j \equiv \sigma \bar{\alpha}_j x - \sigma^2 \bar{s}_j t, \quad Z_j \equiv \sigma \bar{\beta}_j z, \tag{3.5}$$

where Re denotes the real part, x_v and x_1 are defined in (2.1) and (2.3), and ϵ_{2d}, δ_{3d} and δ_{02} are given in (2.9). Since $\bar{s}_j$, $\bar{\alpha}_j$ and $\bar{\beta}_j$ are real X_j and Z_j are real, but we allow the oblique-mode amplitude $\tilde{A}_j$ and the plane-wave amplitude $\tilde{B}_j$ of the jth resonant-triad to be

complex. The mean flow pressure P is a function of x in general and the pressure gradient dP/dx that is equal to μ/R_Δ is scaled by (2.4). The last unsteady term in (3.1) is induced by nonlinear effects in the critical layer. We are interested in the case when the amplitudes of the oblique modes with positive and negative propagation angles are the same. The pair of oblique modes with the same amplitude forms a standing three-dimensional wave that propagates only in the streamwise direction.

The mode shapes $\ddot{\hat{\Phi}}_j$ and Φ_j satisfy the Rayleigh's equations to the required levels of approximation

$$(U - \hat{c}_j)(D^2 - \hat{\gamma}_j^2)\hat{\Phi}_j - U''\hat{\Phi}_j = 0, \tag{3.6}$$

and the complex wavenumbers α_j and γ_j and phase speeds $\ddot{c}_j$ and c_j are given to the required order of approximation by

$$\hat{\gamma}_j = \sigma\left(\bar{\bar{\gamma}}_j + \sigma^r \frac{\bar{\alpha}_j \hat{A}_j'}{\mathrm{i}k\bar{\bar{\gamma}}_j \hat{A}_j}\right), \quad \hat{c}_j = \frac{\sigma \bar{c}_j}{1 + \sigma^r k \hat{A}_j'/(\mathrm{i}\bar{\alpha}_j \hat{A}_j)}, \tag{3.7}$$

where the prime denotes differentiation with respect to the relevant argument, $D \equiv \partial/\partial y$, and $\{\hat{A}_j, \hat{\Phi}_j, \hat{c}_j, \hat{\gamma}_j, \bar{\bar{\gamma}}_j, k\}$ can denote either $\{\tilde{B}_j, \ddot{\hat{\Phi}}_j, \ddot{c}_j, \alpha_j, \bar{\alpha}_j, 1\}$ for the two-dimensional wave or $\{\tilde{A}_j, \Phi_j, c_j, \gamma_j, \bar{\gamma}_j, 2\}$ for the oblique modes. We define $\bar{\gamma}_j$ as

$$\bar{\gamma}_j \equiv \left[(\bar{\alpha}_j/2)^2 + \bar{\beta}_j^2\right]^{1/2}. \tag{3.8}$$

Instead of solving (3.6) with the leading-order inviscid wall boundary condition (Goldstein & Lee 1992; Wundrow *et al.* 1994; Lee 1997a), we will appropriately match the solution of (3.6) with that of the viscous Stokes layer.

By substituting (3.1) – (3.4) into the continuity and momentum equations we can show that (Goldstein & Lee 1992) $\tilde{U}_j$, $\tilde{W}_j$, $\tilde{P}_j$ and $\bar{P}_j$ can be expressed in terms of Φ_j, $D\Phi_j$, $\ddot{\hat{\Phi}}_j$

and $D\ddot{\Phi}_j$ as

$$\tilde{U}_j = \left[D\Phi_j + \frac{4\bar{\beta}_j^2 U'\Phi_j}{\bar{\alpha}_j^2(U-c_j)}\right]\frac{\bar{\alpha}_j}{2\bar{\gamma}_j} + \sigma^r\left[D\Phi_j - \frac{U'\Phi_j}{U-c_j}\left(1+\frac{4\bar{\gamma}_j^2}{\bar{\alpha}_j^2}\right)\right]\frac{\bar{\beta}_j^2 A_j'}{\bar{\gamma}_j^3 \mathrm{i}A_j}, \tag{3.9}$$

$$\tilde{W}_j = -\tfrac{1}{2}\left(\tilde{U}_j - 2\bar{\gamma}_j D\Phi_j/\bar{\alpha}_j\right)\bar{\alpha}_j/\bar{\beta}_j - \sigma^r\left(\tilde{U}_j - \tfrac{1}{2}\bar{\alpha}_j D\Phi_j/\bar{\gamma}_j\right)A_j'/(\bar{\beta}_j \mathrm{i}A_j), \tag{3.10}$$

$$\tilde{P}_j = \gamma_j U'\Phi_j/(\gamma_j^2-\beta_j^2)^{1/2} - (U-c_j)\,\tilde{U}_j, \tag{3.11}$$

$$\tilde{P}_j = U'\ddot{\Phi}_j - (U-\ddot{c}_j)\,D\ddot{\Phi}_j. \tag{3.12}$$

When $r > 1$, the mean flow $U(y, x_v)$ can be written as (Goldstein & Lee 1992; Mankbadi *et al.* 1993; Wundrow *et al.* 1994; Lee 1997a)

$$U = U_B + \sigma^{r-1}\bar{U}_p + \bar{\tilde{U}}(y, x_v) \quad \text{for} \quad y = O(1), \tag{3.13}$$

where U_B is the Blasius velocity and $\sigma^{r-1}\bar{U}_p$ is a small correction due to the pressure gradient. As y approaches the wall, which is assumed to be located at $y = 0$,

$$U_B \to \tau_o y - \frac{\tau_o^2}{2\cdot 4!}y^4 + \frac{11\tau_o^3}{4\cdot 7!}y^7 + \ldots, \quad \bar{U}_p \to \bar{\mu}\left(-\bar{\tau}y + \frac{1}{2}y^2 + \ldots\right), \tag{3.14}$$

where the constant $\tau_o(\simeq 0.332)$ denotes the scaled Blasius skin friction and $\bar{\mu}$ was defined in (2.4). The total wall-shear stress τ_w that is the sum of the Blasius skin friction and the correction due to the mean pressure gradient can be written as (Wundrow *et al.* 1994)

$$\tau_w = \tau_o - \sigma^{r-1}\bar{\mu}\bar{\tau}. \tag{3.15}$$

When $0 < r \leqslant 1$, the correction term due to the pressure gradient is not small any more since the magnitude of the mean pressure gradient μ could be of order one as in (2.4). Therefore, (3.14) and (3.15) should be replaced by (Wu 1993)

$$U \to \tau_w y + \tfrac{1}{2}\mu y^2 + \ldots \quad \text{as} \quad y \to 0. \tag{3.16}$$

In the following analysis $\bar{\mu}$ will be treated as an order-one quantity. However, the results will also be valid for $0 < r \leqslant 1$ if $\bar{\mu}$ is replaced by $\sigma^{1-r}\mu$.

The terms $\bar{\bar{U}}(y, x_v)$ and $V(y, x_v)$ in (3.13) and (3.2), which are functions of the long viscous scale x_v given by (2.1), are included due to the slow viscous spreading of the base mean flow and they can be found by expanding the mean flow solution about $x = 0$. However, they do not make any major contribution to the unsteady flow over the entire streamwise region in which the nonlinear interaction takes place since the local Reynolds number is assumed to be sufficiently large.

As in Goldstein *et al.* (1987), Goldstein & Lee (1992), Wundrow *et al.* (1994), Lee (1997a), and others, the matching can be simplified by using the Miles' (1962) solution, which is obtained by transforming (3.6) into a Riccati equation, and the classical inviscid function (Lin 1955). The latter is written as

$$\hat{\mathcal{W}}_j \equiv \frac{\hat{c}_j D\hat{\Phi}_j}{U'\hat{\Phi}_j - (U - \hat{c}_j)D\hat{\Phi}_j}, \tag{3.17}$$

where $\hat{\mathcal{W}}_j$ can denote either $\ddot{\mathcal{W}}_j$ for the plane wave or $\mathcal{W}_j$ for the oblique modes. Substituting the solution by Miles (1962) along with (3.7) into (3.17), expanding for small σ, and using (3.13) to (3.16) as in Goldstein & Lee (1992), we obtain

$$\begin{aligned}\hat{\mathcal{W}}_j = {} & \frac{\bar{c}_j U'}{\bar{\bar{\gamma}}_j(1-\sigma\bar{c}_j)^2} - \frac{\sigma\bar{c}_j\tau_w}{(1-\sigma\bar{c}_j)^4}\left(J_1 + \sigma 2\bar{c}_j J_2 + \sigma^2\bar{c}_j^2 J_3 + \frac{y^2}{8\tau_w}\right) + \sigma^2\bar{\bar{\gamma}}_j\bar{c}_j\tau_w(2J_4 + \sigma\bar{c}_j J_5) \\ & -\sigma^2\frac{\bar{c}_j^2}{4\tau_w}y - \sigma^3\frac{7\bar{c}_j^3}{48\tau_w^2} + \sigma^r\frac{\bar{c}_j}{\tau_w^2}\left(\tfrac{3}{2}\bar{\mu} + \bar{\mu}_{cj}\ln y\right) + \sigma^r\frac{\mathrm{i}\bar{c}_j\tau_w}{\bar{\bar{\gamma}}_j^2}\left(\frac{\bar{\alpha}_j}{k\bar{\bar{\gamma}}_j} + \frac{k\bar{\bar{\gamma}}_j}{\bar{\alpha}_j}\right)\frac{\hat{A}_j'}{\hat{A}_j} + \ldots,\end{aligned} \tag{3.18}$$

where the constants J_1 to J_5 are given in Appendix A of Lee (1997a) and we have put

$$\bar{\mu}_{cj} \equiv \bar{\mu} - \sigma^{3-r}\left(\tfrac{1}{2}\tau_o Y_{cj}\right)^2. \tag{3.19}$$

We have also used the fact that

$$\bar{c}_j = \tau_w Y_{cj} + \sigma^r \tfrac{1}{2} Y_{cj}^2 \left(\bar{\mu} - \sigma^{3-r} \tau_o^2 Y_{cj}^2 / 4! \right) + \ldots, \tag{3.20}$$

which is obtained from (2.2), (2.7) and (3.13) – (3.16). The above equation (3.20) determines Y_{cj} once $\bar{c}_j$ is known.

4. The viscous Stokes layer

As shown in Goldstein & Lee (1992), Wundrow *et al.*, (1994) and Lee (1997a), the viscous Stokes layer adjacent to the wall does not make a leading-order contribution to the growth of the instability wave in the non-equilibrium critical-layer analysis. This thin viscosity dominated layer, however, produces an order-one growth term when the Tollmien-Schlichting waves are considered as in the quasi-equilibrium analyses by Mankbadi *et al.* (1993) and Wu (1993). It was pointed out by Wu *et al.* (1993) and shown in detail by Lee (1997a) that the quasi-equilibrium amplitude equations of Mankbadi *et al.* (1993) and Wu (1993) can be alternatively derived by taking the viscous limit of the finite-viscosity amplitude equations provided the viscous Stokes layer effect is appropriately included in the the linear growth rates. Goldstein & Lee (1992, 1993) identified these correction terms by comparing their results with those of the quasi-equilibrium critical-layer analyses. In this section, the unsteady flow in the viscous Stokes layer will be analyzed in order to obtain, in a systematic way, the linear growth rate of the instability wave that is also valid in the viscous limit.

The generalized scaling by Lee (1997a) shows that the viscous Stokes layer for the

non-equilibrium critical-layer analysis is scaled as

$$y = \sigma^{3r/2+1}\hat{y}. \tag{4.1}$$

If we substitute (3.1) – (3.4), (4.1) and

$$\hat{\Phi}_j = \sigma^{3r/2+1}\hat{\tilde{\Phi}}_j, \tag{4.2}$$

into the continuity and momentum equations, we can obtain

$$\lambda\hat{\tilde{\Phi}}_{j\hat{y}^4} + \frac{\mathrm{i}\bar{\alpha}_j}{k}\left(\bar{c}_j - \frac{U}{\sigma}\right)\hat{\tilde{\Phi}}_{j\hat{y}\hat{y}} = 0, \tag{4.3}$$

where $\{\hat{\tilde{\Phi}}_j, \hat{\Phi}_j, k\}$ can denote either $\{\ddot{\tilde{\Phi}}_j, \ddot{\Phi}_j, 1\}$ for the plane wave or $\{\tilde{\Phi}_j, \Phi_j, 2\}$ for the oblique modes and the base mean flow U is given by (3.13) to (3.16). The bounded solution which satisfies the no-slip boundary condition at the wall ($\hat{y} = 0$) is

$$\hat{\tilde{\Phi}}_j = \sigma^{-(3r/2+1)}U + (\tau_w/\hat{b}_j)\left(e^{-\hat{b}_j\hat{y}} - 1\right), \tag{4.4}$$

where

$$1/\hat{b}_j = (1+\mathrm{i})\left(\tfrac{1}{2}k\lambda/\bar{s}_j\right)^{1/2}. \tag{4.5}$$

It is easy to show from (4.4) that

$$\hat{\tilde{\Phi}}_j \to \sigma^{-(3r/2+1)}U - \tau_w/\hat{b}_j \quad \text{as} \quad \hat{y} \to \infty. \tag{4.6}$$

This will be matched with the inviscid wall layer solution in the following section.

5. The inviscid wall layer

The analyses of Graebel (1966) and Nield (1972) suggest that we have to introduce the scaled transverse coordinate

$$Y \equiv y/\sigma \tag{5.1}$$

directly into (3.6) before attempting to obtain the solution. The solution is of the form

$$\hat{\Phi}_j = \sigma\tau_w Y + \sigma^{r+1} F_j(Y, \hat{\phi}_j^{\pm}) + \ldots, \tag{5.2}$$

where the integration constant $\hat{\phi}_j^{\pm}$, which can denote either $\ddot{\phi}_j^{\pm}$ or $\phi_j^{\pm}$ for the plane or oblique waves respectively, is a complex function of x_1 in general. Matching (5.2) with the viscous Stokes-layer solution (4.6), along with (3.13) - (3.16), (4.1), (4.2) and (5.1), shows that F_j must satisfy

$$F_j \to -\sigma^{r/2}\tau_w/\hat{b}_j \quad \text{as} \quad Y \to 0, \tag{5.3}$$

where $\hat{b}_j$ is given by (4.5).

We can show that F_j, which satisfies the above matching condition and can be discontinuous across the critical level Y_{cj}, is given by

$$F_j^{\pm} = f_j(Y) + \mathrm{i}\bar{\mu}_{cj} Y_{cj} \left[(Y - Y_{cj})\hat{\phi}_j^{\pm} + Y_{cj}\hat{\phi}_j^{-}\right] - \sigma^{r/2}\tau_w/\hat{b}_j + \ldots, \quad \text{for} \quad Y \gtrless Y_{cj}, \tag{5.4}$$

where

$$f_j(Y) = \bar{\mu}_{cj}\left[\tfrac{1}{2}Y^2 + Y_{cj}\left\{(Y - Y_{cj})\ln|Y - Y_{cj}| + Y_{cj}\ln Y_{cj}\right\}\right] - \sigma^{3-r}\tau_o^2 Y^3\left(Y_{cj} + \tfrac{1}{2}Y\right)/4!, \tag{5.5}$$

and $\bar{\mu}_{cj}$ is given by (3.19). The last term in (5.4) was added due to the effect of the viscous Stokes layer and becomes $(1+\mathrm{i})\tau_w\left(\frac{1}{2}k\sigma^r\lambda/\bar{s}_j\right)^{1/2}$ if we substitute (4.5). Its magnitude is of higher order, i.e. $O(\sigma^{r/2})$, in the present finite-viscosity case, but it will be of order one in the viscous-limit (quasi-equilibrium critical-layer) case where λ becomes $O(\sigma^{-r})$. The rescaling of λ in the viscous limit will be given in Part 2 (also by (8.8) of Lee (1997a)). It is obvious that we need to include more (inviscid) terms (Wundrow *et al.* 1994) on the right hand side of (5.4) in order to make that to be uniformly valid up to $O(\sigma^{r/2})$. However, in

the following analysis, we will keep the viscous correction term as in (5.4) and treat it as if the magnitude of $\sigma^r\lambda$ is of order one since we are mostly interested in the leading-order effect of that term in the viscous limit.

In the later non-equilibrium critical-layer stage, r becomes smaller than 3 as summarized in table 1 of Lee (1997a) and $\bar{\mu}$ is also likely to become negligibly small as in Wundrow *et al.* (1994). Thus, $\bar{\mu}_{cj}$ defined in (3.19) becomes negligibly small so does the linear velocity jump across the critical layer. When $\bar{\mu}_{cj} \ll 1$, (5.4) can be explicitly rewritten as

$$F_j^{\pm} = f_j(Y) + \mathrm{i}\bar{\mu}_{cj}Y_{cj}\left[(Y-Y_{cj})\left(\hat{\phi}_j^{(N)\pm} + \bar{\mu}_{cj}\hat{\phi}_j^{(L)\pm}\right) + Y_{cj}\left(\hat{\phi}_j^{(N)-} + \bar{\mu}_{cj}\hat{\phi}_j^{(L)-}\right)\right] \\ -\sigma^{r/2}\tau_w/\hat{b}_j + \ldots, \quad \text{for} \quad Y \gtrless Y_{cj}, \quad (5.6)$$

where $\hat{\phi}_j^{(N)\pm}$ accounts for the $O(1)$ nonlinear jump while $\bar{\mu}_{cj}\hat{\phi}_j^{(L)\pm}$ accounts for the very small linear jump. However, for the simplicity, we will treat $\bar{\mu}_{cj}$ as an $O(1)$ quantity and (5.4) will be used instead of (5.6) in the following analysis. The result will be still valid even when $\bar{\mu}_{cj} \ll 1$ if $\bar{\mu}_{cj}\hat{\phi}_j^{\pm}$ is simply replaced by $\hat{\phi}_j^{(N)\pm} + \bar{\mu}_{cj}\hat{\phi}_j^{(L)\pm}$.

Inserting (3.13) – (3.16), (5.1), (5.2), (5.4) and (5.5) into (3.17) and re-expanding, we obtain

$$\hat{\mathcal{W}}_j = \frac{U'}{\tau_w} + \sigma^r\frac{\bar{\mu}_{cj}Y_{cj}^2}{\bar{c}_j}\left[\ln\frac{Y-Y_{cj}}{Y_{cj}} - \mathrm{i}\left(\hat{\phi}_j^- - \hat{\phi}_j^+\right)\right] - \sigma^3\tfrac{1}{4}\bar{c}_jY\left(Y_{cj} + \tfrac{1}{2}Y\right) + \sigma^{3r/2}\frac{\tau_w}{\bar{c}_j\hat{b}_j} + \ldots, \quad (5.7)$$

for $Y > Y_{cj}$. The inviscid function (5.7) in the inviscid wall layer will be matched with that in (3.18) obtained in the main boundary layer as explained below.

The (linear) real part of the wavenumber of the jth resonant-triad $\bar{\alpha}_j$ in (2.2) possesses a power-series expansion

$$\bar{\alpha}_j = \bar{\alpha}_j^{(0)} + \sigma\bar{\alpha}_j^{(1)} + \sigma^2\bar{\alpha}_j^{(2)} + \ldots + \sigma^r(\ln\sigma)\bar{\alpha}_j^{(rL)} + \sigma^r\bar{\alpha}_j^{(r)} + \ldots. \quad (5.8)$$

Matching (5.7) with (3.18) along with (2.5), (3.13) – (3.16), (4.5) and (5.1) for the jth plane wave where $\{\hat{A}_j, \bar{\bar{\gamma}}_j, \hat{\phi}_j^{\pm}, k\}$ must be replaced by $\{\tilde{B}_j, \bar{\alpha}_j, \ddot{\phi}_j^{\pm}, 1\}$ shows that (Goldstein & Lee 1992; Wundrow *et al.* 1994; Lee 1997a), for $0 < r \leqslant 3$,

$$\bar{\alpha}_j^{(0)} = (\tau_w \bar{s}_j)^{1/2}, \tag{5.9}$$

$$\bar{\alpha}_j^{(1)} = \bar{s}_j(1 - \tfrac{1}{2}\tau_w J_1) \quad \text{if} \quad r > 1, \tag{5.10}$$

$$\bar{\alpha}_j^{(2)} = -\tfrac{1}{2}\bar{s}_j(\tau_w \bar{s}_j)^{1/2}\left[3J_1 + 2J_2 - \tfrac{1}{4}\tau_w(J_1^2 + 8J_4)\right] \quad \text{if} \quad r > 2, \tag{5.11}$$

$$\bar{\alpha}_j^{(rL)} = \tfrac{1}{2}\bar{\mu}\bar{s}_j/\tau_w^2 - \sigma^{[3-r]}\tfrac{1}{8}(Y_{cj}\bar{\alpha}_j)^2/\tau_w, \tag{5.12}$$

$$\bar{\alpha}_j^{(r)} = \tfrac{1}{2}(\tfrac{3}{2} + \ln Y_{cj})\bar{\mu}\bar{s}_j/\tau_w^2 - \tfrac{1}{2}(\bar{\alpha}_j/\bar{c}_j)^2\left(\tfrac{1}{2}\sigma^r\lambda/\bar{s}_j\right)^{1/2} - \sigma^{[3-r]}\tfrac{1}{2}\bar{s}_j^2\left[\left(3 + 2\tau_w^2 J_4\right)J_1 + 4J_2 + J_3 - \tau_w J_5 + \left\{7/48 + \tfrac{1}{4}(\tau_w Y_{cj}/\bar{c}_j)^2 \ln Y_{cj}\right\}/\tau_w^3\right] + \sigma^{[2-r]}\bar{\alpha}_j^{(2)} + \sigma^{[1-r]}\bar{\alpha}_j^{(1)}, \tag{5.13}$$

and

$$\frac{\tilde{B}_j'}{\tilde{B}_j} = -\frac{\bar{\alpha}_j^2}{2\bar{c}_j^2}\left[\frac{\bar{\mu}_{cj}Y_{cj}^2}{\tau_w}\left(\ddot{\phi}_j^- - \ddot{\phi}_j^+\right) - \left(\frac{\sigma^r\lambda}{2\bar{s}_j}\right)^{1/2}\right], \tag{5.14}$$

where $\sigma^{[n-r]}$ is defined to be equal to σ^{n-r} if $n \geqslant r$ or equal to zero when $n < r$, $\bar{\mu}_{cj}$ is given by (3.19) and J_1 to J_5 are given in Appendix A of Lee (1997a).

The above equations (5.9) – (5.13) are the usual long-wavelength small-growth-rate dispersion relations that determine the wavenumber $\bar{\alpha}_j$ in terms of $\bar{s}_j$. The phase speed $\bar{c}_j$ which possesses a similar expansion to (5.8) is determined by (2.5). The complex plane wave amplitude $\tilde{B}_j$ of the j resonant-triad is determined by the phase-jump equation (5.14). The effect of the viscosity now appears as the second term on the right hand side of (5.14) and always increases the growth rate. The phase jump $\ddot{\phi}_j^- - \ddot{\phi}_j^+$ across the critical layer can be obtained by considering the critical layer and is equal to the sum of $-\pi$ and a complex function of x_1 as will be shown in §6 (Drazin & Reid 1981; Goldstein & Lee 1992).

The former and the real part of the latter represent the linear and nonlinear growth rates, respectively, while the nonlinear correction of the wavenumber is given by the imaginary part of the latter. The linear part of the wavenumber, $\bar{\alpha}_j$ has been fully determined, up to the order of σ^r, by matching as given by (5.8) - (5.13) (Wundrow *et al.* 1994).

As shown above, $\bar{\alpha}_j$ and $\bar{c}_j$ have been determined from the matching of the plane-wave inviscid functions. The wavenumber $\bar{\gamma}_j$ can now be determined by matching the inviscid functions of the oblique modes. It is convenient to put

$$\bar{\beta}_j = \tfrac{\sqrt{3}}{2}(\bar{\alpha}_j + \sigma^r \kappa_s), \tag{5.15}$$

and then from (3.8)

$$\bar{\gamma}_j = \bar{\alpha}_j + \sigma^r \tfrac{3}{4}\kappa_s + \ldots, \tag{5.16}$$

where κ_s will be determined from matching. By matching (5.7) with (3.18) along with (2.5), (3.13) - (3.16), (4.5), (5.1) and (5.16) and replacing $\{\hat{A}_j, \bar{\tilde{\gamma}}_j, \hat{\phi}_j^{\pm}, k\}$ by $\{\tilde{A}_j, \bar{\gamma}_j, \phi_j^{\pm}, 2\}$ for the oblique modes, we can show that

$$\left(\frac{\bar{\alpha}_j}{2\bar{\gamma}_j} + \frac{2\bar{\gamma}_j}{\bar{\alpha}_j}\right)\frac{\tilde{A}_j'}{\tilde{A}_j} = -\frac{\bar{\gamma}_j^2}{\bar{c}_j^2}\left[\frac{\bar{\mu}_{cj} Y_{cj}^2}{\tau_w}\left(\phi_j^- - \phi_j^+\right) - \left(\frac{\sigma^r \lambda}{\bar{s}_j}\right)^{1/2}\right] + \mathrm{i}\kappa_{vj}, \tag{5.17}$$

where κ_{vj} appears due to the viscous Stokes-layer effect. Since we have chosen κ_s in (5.15) to be the same for all j, which we put

$$\kappa_s = \tfrac{4}{3}\left(\tfrac{1}{\sqrt{2}} - 1\right)(\sigma^r \lambda/\bar{s}_0)^{1/2}(\bar{\alpha}_0/\bar{c}_0)^2, \tag{5.18}$$

the higher-order j-dependent correction term κ_{vj} must be included in (5.17),

$$\kappa_{vj} = \left(\tfrac{1}{\sqrt{2}} - 1\right)(\sigma^r \lambda)^{1/2}(\bar{\gamma}_j/\bar{\alpha}_j)\left[\bar{\alpha}_j\bar{\gamma}_j/(\bar{c}_j^2 \bar{s}_j^{1/2}) - \bar{\alpha}_0^2/(\bar{c}_0^2 \bar{s}_0^{1/2})\right]. \tag{5.19}$$

Using (2.6), (5.16), (5.21) and (5.22), we can show that the magnitude of κ_{vj} is of the order of $\sigma^r(\sigma^r\lambda)^{1/2}$. The phase jump $\phi_j^- - \phi_j^+$ is equal to $-\pi$ (for the linear growth rate) plus

a complex function of x_1 (whose real and imaginary parts represent the nonlinear growth rate and the nonlinear wavenumber correction, respectively).

It is easy to show from (3.1) and (3.5) that the nonlinearly corrected streamwise wavenumber of the oblique mode becomes $\sigma\bar{\alpha}_j/2 - \sigma^{r+1}\mathrm{Re}i\tilde{A}'_j/\tilde{A}_j$. Thus, the nonlinear propagation angle of the jth oblique modes, $\pm\tilde{\theta}_j$ can be computed, up to $O(\sigma^r)$, by

$$\tilde{\theta}_j = \tan^{-1}\left(\frac{\bar{\beta}_j}{\bar{\alpha}_j/2 - \sigma^r \mathrm{Re}i\tilde{A}'_j/\tilde{A}_j}\right), \tag{5.20}$$

where $\bar{\alpha}_j$ and $\bar{\beta}_j$ can be evaluated from (5.8) – (5.13), (5.15) and (5.18). As we expected (Goldstein & Lee 1992), $\tilde{\theta}_j$ becomes $\pi/3$ at the leading order.

The result presented so far is basically a linear superposition of the (modified) results of the single-resonant-triad analyses by Goldstein & Lee (1992) and Lee (1997a) since the unsteady flows in the main boundary layer, viscous Stokes layer and inviscid wall layer are governed by the linear dynamics to the required order of approximation.

From (2.5), (3.19), (3.20), (5.8) – (5.13), (5.15), (5.16) and (5.18), the quantities of the jth resonant-triad can be expressed in terms of the 'reference' 0th resonant-triad, when $\bar{s}_j$ is given by (2.6),

$$\bar{\alpha}_j = \bar{\alpha}(1 + \sigma^r \tfrac{1}{2} j\tilde{\chi}), \quad \bar{\beta}_j = \bar{\beta} + \sigma^r \tfrac{\sqrt{3}}{4} j\tilde{\chi}\bar{\alpha}, \quad \bar{\gamma}_j = \bar{\gamma} + \sigma^r \tfrac{1}{2} j\tilde{\chi}\bar{\alpha} + \ldots, \tag{5.21}$$

$$\bar{c}_j/\bar{c} = 1 + \sigma^r \tfrac{1}{2} j\chi + \ldots, \quad Y_{cj}/Y_c = 1 + \sigma^r \tfrac{1}{2} j\chi + \ldots, \quad \bar{\mu}_{cj} = \bar{\mu}_c + O(\sigma^3), \tag{5.22}$$

where

$$\tilde{\chi} = \chi\left(1 + \sigma\bar{\alpha}^{(1)}/\bar{\alpha} + \sigma^2 2\bar{\alpha}^{(2)}/\bar{\alpha} + \ldots\right), \tag{5.23}$$

and $\bar{\alpha}^{(1)}$ and $\bar{\alpha}^{(2)}$ are given by (5.10) and (5.11). We have omitted in the above equations and we will omit in the rest of this paper the subscript 0 for the quantities of the 'reference' 0th resonant-triad for notational simplicity.

It is convenient to introduce the slow time t_1 and the slow spanwise coordinate z_1 which are defined as

$$t_1 = \sigma^{r+2}\chi\bar{s}t, \quad z_1 = \sigma^{r+1}\tfrac{\sqrt{3}}{4}\tilde{\chi}\bar{\alpha}z. \tag{5.24}$$

By using (2.6), (5.21) and (5.24), we can show that $X_\jmath$ and $Z_\jmath$ defined in (3.5) become

$$X_\jmath = X - \jmath t_1 + \tfrac{1}{2}\jmath\tilde{\chi}\bar{\alpha}x_1, \quad Z_\jmath = Z + \jmath z_1. \tag{5.25}$$

If we put

$$\bar{A}_\jmath(x_1) = \tilde{A}_\jmath(x_1)e^{i\jmath\tilde{\chi}\bar{\alpha}x_1/4}, \quad \bar{B}_\jmath(x_1) = \tilde{B}_\jmath(x_1)e^{i\jmath\tilde{\chi}\bar{\alpha}x_1/2}, \tag{5.26}$$

and use (5.19), (5.21) and (5.22), the phase-jump equations (5.17) and (5.14) can be rewritten as, for $-J \leqslant \jmath \leqslant J$,

$$\left(\cos\theta + \frac{1}{\cos\theta}\right)\left(\frac{\bar{A}'_\jmath}{\bar{A}_\jmath} - \frac{\mathrm{i}}{4}\jmath\tilde{\chi}\bar{\alpha}\right) = -\frac{\bar{\gamma}^2}{\bar{c}^2}\left[\frac{\bar{\mu}_c Y_c^2}{\tau_w}\left(\phi_\jmath^- - \phi_\jmath^+\right) - \left(\frac{\sigma^r\lambda}{\bar{s}}\right)^{1/2}\right], \tag{5.27}$$

$$\frac{\bar{B}'_\jmath}{\bar{B}_\jmath} - \frac{\mathrm{i}}{2}\jmath\tilde{\chi}\bar{\alpha} = -\frac{\bar{\alpha}^2}{2\bar{c}^2}\left[\frac{\bar{\mu}_c Y_c^2}{\tau_w}\left(\ddot{\phi}_\jmath^- - \ddot{\phi}_\jmath^+\right) - \left(\frac{\sigma^r\lambda}{2\bar{s}}\right)^{1/2}\right], \tag{5.28}$$

where $\bar{\mu}_c$ for the 0th resonant-triad is given by (3.19) and θ is defined as

$$\theta \equiv \cos^{-1}\left(\tfrac{1}{2}\bar{\alpha}/\bar{\gamma}\right), \tag{5.29}$$

which is the same, but $\sigma^r \mathrm{Re} i\tilde{A}'_\jmath/\tilde{A}_\jmath$, as the nonlinear propagation angle $\tilde{\theta}$ in (5.20) when $\jmath = 0$. The relation (5.16) shows that θ is $\pi/3$ at the leading order, but it can be fully determined because $\bar{\alpha}$ and $\bar{\gamma}$ are known from (5.8) to (5.13), (5.16) and (5.18).

The phase jumps across the critical layer will be determined from the nonlinear analysis within the critical layer. Since we are interested in the instability waves that are spatially growing in the streamwise direction in the linear upstream region, they will continue to grow only in the streamwise direction as they propagate downstream. The amplitudes $\bar{A}_\jmath$

and $\bar{B}_j$ are complex functions of x_1 but are independent of t_1 and z_1. The wavetrains (Wu, Stewart & Cowley 1996) which can grow in the slow time and in the spanwise direction will be considered in a subsequent paper.

Equations (5.1), (5.2), (5.4), (5.5), (5.21) - (5.23) along with (3.9) - (3.16) show that (3.1) - (3.4) can be rewritten in this inviscid Tollmien region as (Goldstein & Lee 1992; Lee 1997a),

$$u = \sigma\tau_w Y + \sigma^{r+1}\tfrac{1}{2}\bar{\mu}Y^2 - \sigma^4\frac{\tau_o^2}{2\cdot 4!}Y^4 + \epsilon_{2d}\sum_{j=-J}^{J}\mathrm{Re}\left[\tau_w + \sigma^r\left(f_Y + \mathrm{i}\bar{\mu}_c Y_c\ddot{\phi}_j^{\pm}\right)\right]\bar{B}_j\tilde{E}_j$$

$$+\delta_{3d}\sum_{j=-J}^{J}2\tau_w(\sec\theta)\mathrm{Re}\left\{1+\zeta(\sin^2\theta)\left[1+\sigma^r\tfrac{1}{2}j\chi(1+\zeta)\right]+\sigma^r\frac{\zeta}{\bar{c}}(\sin^2\theta)\left[f+\frac{\bar{c}f_Y}{\tau_w\zeta\tan^2\theta}\right.\right.$$

$$+\tfrac{1}{2}\bar{\mu}Y^2(1-\zeta)-\sigma^{3-r}\frac{\tau_o^2Y^4}{2\cdot 4!}(3-\zeta)-\frac{\bar{c}\bar{A}_j'}{\mathrm{i}\bar{\gamma}\bar{A}_j}\left(\cos\theta+\frac{\tau_w^2Y^2\zeta}{\bar{c}^2\cos\theta}\right)+\frac{\mathrm{i}\bar{c}\bar{\mu}_cY_c}{\tau_w}\left(\phi_j^- + \frac{\phi_j^{\pm}}{\zeta\sin^2\theta}\right)$$

$$\left.\left.-(1+\mathrm{i})\tau_w\left(\frac{\sigma^r\lambda}{\bar{s}}\right)^{1/2}\right]\right\}\bar{A}_j\tilde{E}_{cj}+\delta_{02}\sum_{j=-2J}^{2J}\sum_{\ell}\mathrm{Re}\,\bar{\bar{U}}_{0,2;j,\ell}e^{-\mathrm{i}jt_1/2}\cos[2Z+(j+2\ell)z_1]$$

$$+\ldots, \quad (5.30)$$

$$v = -\sigma^2\sum_{j=-J}^{J}\mathrm{Re}\left[\epsilon_{2d}\left\{\tau_wY+\sigma^r\mathrm{i}\bar{\mu}_cY_c(Y-Y_c)\ddot{\phi}_j^{\pm}+\ldots\right\}\mathrm{i}\bar{\alpha}\bar{B}_j\tilde{E}_j\right.$$

$$\left.+\delta_{3d}\left\{\tau_wY+\sigma^r\mathrm{i}\bar{\mu}_cY_c(Y-Y_c)\phi_j^{\pm}+\ldots\right\}2\mathrm{i}\bar{\gamma}\bar{A}_j\tilde{E}_{cj}\right]+\ldots, \quad (5.31)$$

$$w = -\delta_{3d}\sum_{j=-J}^{J}2(\sin\theta)\mathrm{Re}\mathrm{i}\tau_w\zeta\bar{A}_j\tilde{E}_{sj}+\ldots, \quad (5.32)$$

$$p = P+\sum_{j=-J}^{J}\sigma\bar{c}\tau_w\mathrm{Re}\left[\epsilon_{2d}\bar{B}_j\tilde{E}_j+\delta_{3d}2(\cos\theta)\bar{A}_j\tilde{E}_{cj}\right]+\ldots, \quad (5.33)$$

where ϵ_{2d}, δ_{3d} and δ_{02} are given by (2.9), f and $\bar{\mu}_c$ are given by (5.5) and (3.19) and we have put

$$\tilde{E}_j \equiv e^{\mathrm{i}(X-jt_1)}, \quad \tilde{E}_{cj}\equiv e^{\mathrm{i}(X-jt_1)/2}\cos(Z+jz_1), \quad \tilde{E}_{sj}\equiv e^{\mathrm{i}(X-jt_1)/2}\sin(Z+jz_1), \quad (5.34)$$

and

$$\zeta \equiv \bar{c}/(\tau_wY-\bar{c}). \quad (5.35)$$

In the streamwise velocity (5.30), the term $\sigma^r \frac{1}{2} \jmath \chi (1 + \zeta)$ appears because the quantities of the $\jmath$th resonant-triad are expanded about those of the 0th resonant-triad as in (5.21) – (5.23) and the term which is proportional to $(\sigma^r \lambda / \bar{s})^{1/2}$ is included due to the viscous Stokes layer effect. The last term on the right hand side of (5.30) that is a function of the slow time t_1 is included in order to match with the critical-layer solution. The $O(\sigma^{r+2})$ terms that are continuous across the critical layer are not shown in (5.31) since they do not play any major role in the analysis. The mean pressure is denoted by P in (5.33). The above solutions have to be rescaled in the critical layer since they become singular at $Y = Y_c$.

Although we have used the non-equilibrium critical-layer scaling given in §2, the results in this section as well as in §3 and §4 are also valid in the viscous limit since the leading-order viscosity effect was included by considering the viscous Stokes layer. In the viscous limit where λ defined in (2.8) is of $O(\sigma^{-r})$, see (8.8) of Lee (1997a), the critical layer becomes of the quasi-equilibrium type and the viscous Stokes layer becomes thicker (Mankbadi *et al.* 1993; Wu 1993). The generalized scaling given in table 1 and (8.9) of Lee (1997a) indicates that λ, ϵ_{2d}, δ_{3d}, δ_{02} and $\hat{y}$ in (2.8), (2.9) and (4.1) must be rescaled for the quasi-equilibrium critical-layer analysis.

6. The critical layer

The nonlinear analysis of the detuned resonant-triads within the critical layer will be presented in this section. The system of critical-layer equations and jump equations will be derived here and their normalized version will be given in the following section.

The thickness of the non-equilibrium critical layer is of the same order as the growth rate, i.e. $O(\sigma^{r+1})$, as shown by Goldstein *et al.* (1987), Goldstein & Lee (1992), Wundrow

et al. (1994) and Lee (1997a). The growth rate and the linear convection terms become of the same order of magnitude there. The appropriate transverse coordinate in this region is

$$\bar{\eta} = (Y - Y_c)/\sigma^r = (y - y_c)/\sigma^{r+1}. \tag{6.1}$$

The continuity and momentum equations expressed in terms of the scaled variables x_1, X, Z, z_1, t_1 and $\bar{\eta}$, which were defined in (2.3), (3.5), (5.24) and (6.1), become

$$\bar{\alpha}u_X + \bar{v}_{\bar{\eta}} + \bar{\beta}w_Z + \sigma^r\left(u_{x_1} + \tfrac{\sqrt{3}}{4}\tilde{\chi}\bar{\alpha}w_{z_1}\right) = 0, \tag{6.2}$$

$$\bar{D}\{u, \bar{v}, w\} = -\left\{\bar{\alpha}p_X + \sigma^r p_{x_1}, \sigma^{-(2r+4)}p_{\bar{\eta}}, \bar{\beta}p_Z + \sigma^r\tfrac{\sqrt{3}}{4}\tilde{\chi}\bar{\alpha}p_{z_1}\right\}, \tag{6.3}$$

where we have put

$$\bar{D} \equiv \bar{\alpha}(u - \sigma\bar{c})\frac{\partial}{\partial X} + \bar{v}\frac{\partial}{\partial\bar{\eta}} + \bar{\beta}w\frac{\partial}{\partial Z} + \sigma^r\left(u\frac{\partial}{\partial x_1} + \tfrac{\sqrt{3}}{4}\tilde{\chi}\bar{\alpha}w\frac{\partial}{\partial z_1}\right) + \sigma^{r+1}\left(\chi\bar{\alpha}\bar{c}\frac{\partial}{\partial t_1} - \lambda\frac{\partial^2}{\partial\bar{\eta}^2}\right), \tag{6.4}$$

$$v = \sigma^{r+2}\bar{v}. \tag{6.5}$$

The viscous parameter λ is defined by (2.8), the frequency-detuning factor χ is introduced by (2.6), $\tilde{\chi}$ is given by (5.23) and u, v, w and p are total velocities and pressure. The quantities $\bar{\alpha}$, $\bar{\beta}$, $\bar{c}$ and Y_c represent those of the 0th resonant-triad, i.e. when $j = 0$, as mentioned in the previous section.

Putting (2.9) and (6.1) into (5.30) to (5.33) and re-expanding the results show that the critical-layer solution must be of the form

$$u - \sigma\bar{c} = \sigma^{r+1}\tau_w\bar{\eta} + \sigma^{2r+1}u^{(1)} + \sigma^{3r+1}u^{(2)} + \sigma^{4r+1}u^{(3)} + \sigma^{5r+1}u^{(4)} + \ldots, \tag{6.6}$$

$$\bar{v} = -\sigma^{2r+1}\sum_{j=-J}^{J} 2\bar{\gamma}\tau_w Y_c \mathrm{Re}\mathrm{i}\bar{A}_j\tilde{E}_{cj} + \sigma^{3r+1}\bar{v}^{(2)} + \sigma^{4r+1}\bar{v}^{(3)} + \sigma^{5r+1}\bar{v}^{(4)} + \ldots, \tag{6.7}$$

$$w = \sigma^{2r+1}w^{(1)} + \sigma^{3r+1}w^{(2)} + \sigma^{4r+1}w^{(3)} + \sigma^{5r+1}w^{(4)} + \ldots, \tag{6.8}$$

$$p = P + \sigma^{3r+2} \sum_{j=-J}^{J} 2\bar{c}\tau_w(\cos\theta)\mathrm{Re}\,\bar{A}_j\tilde{E}_{cj} + \sigma^{4r+2}p^{(2)} + \sigma^{5r+2}p^{(3)} + \ldots, \tag{6.9}$$

where $\tilde{E}_{cj}$ is defined by (5.34), τ_w is given by (3.15) and θ is defined in (5.29). The solutions in the inviscid Tollmien region (5.30) – (5.33) indicate that we must include the terms $\sigma^{4r+1}(\ln\sigma)u^{(3L)}$ and $\sigma^{5r+1}(\ln\sigma)u^{(4L)}$ into (6.6) and similar terms for $\bar{v}$, w and p into (6.7) – (6.9). However, these logarithmic terms do not play any active role in the present analysis and thus they are omitted for the simplicity. Substituting these expansions (6.6) – (6.9) into (6.2) – (6.5) with (3.15) we can obtain the governing equations for $u^{(l)}$, $\bar{v}^{(l)}$, $w^{(l)}$ and $p^{(l)}$ which are given in Appendix A.

As in previous studies (Goldstein & Lee 1992; Lee 1997a) we can solve these equations (A 1) – (A 11) subject to the transverse boundary conditions that they match onto the outer solutions (5.30) – (5.33). The relevant solutions for the lowest-order are given by

$$u^{(1)} = u_M^{(1)}(\bar{\eta}, x_1) + \sum_{j=-J}^{J} \mathrm{Re}2\mathrm{i}(\tan\theta)\tilde{Q}_j^{(1)}(\bar{\eta}, x_1)\tilde{E}_{cj}, \tag{6.10}$$

$$w^{(1)} = \sum_{j=-J}^{J} \mathrm{Re}2\tilde{Q}_j^{(1)}(\bar{\eta}, x_1)\tilde{E}_{sj}, \tag{6.11}$$

where $\tilde{E}_{sj}$ and $\tilde{E}_{cj}$ are given by (5.34). From (5.30) and (6.6), we can show that the base mean flow component $u_M^{(1)}$ becomes

$$u_M^{(1)} = a_M^{(1)}\bar{\eta}, \tag{6.12}$$

where

$$a_M^{(1)} = \bar{\mu}Y_c - \sigma^{3-r}\tau_o^2 Y_c^3/12 + \ldots. \tag{6.13}$$

However, since the constant $a_M^{(1)}$ is not required to be evaluated in the following analysis, we will retain the general form (6.12) without substituting (6.13).

The nonlinear equations in Appendix A indicate that more Fourier components must be considered in this multi-frequency analysis than in the single-resonant-triad case. We can show that $u^{(2)}$, $u^{(3)}$ and $u^{(4)}$ possess the following expansions:

$$u^{(2)} = u_M^{(2)} + \sum_{\jmath|1} \mathrm{Re}\left\{\left(\tilde{U}_{1,1;\jmath}^{(2L)}\mathcal{E}_{1;\jmath}\right)^\dagger E_{1;\jmath} + \tilde{U}_{2,0;\jmath}^{(2L)} E_{2;2\jmath}\right\} + \sum_{\jmath|2} \mathrm{Re}\left\{\left(\tilde{U}_{0,0;\jmath}^{(2)}\mathcal{E}_{0;\jmath}\right)^\dagger E_{0;\jmath} + \left(\tilde{U}_{2,2;\jmath}^{(2)}\right.\right.$$
$$\left.\left.\mathcal{E}_{2;\jmath}\right)^\dagger E_{2;\jmath} + \sum_{\ell:1}\left(\tilde{U}_{2,0;\jmath,\ell}^{(2)}\mathcal{E}_{0;\jmath-2\ell}\right)^\dagger E_{2;\jmath} + \sum_{\ell:-1}\left(\tilde{U}_{0,2;\jmath,\ell}^{(2)}E_{0;\jmath} + \tilde{U}_{-0,2;\jmath,\ell}^{(2)}E_{0;-\jmath}\right)\mathcal{E}_{2;\jmath+2\ell}\right\}, \quad (6.14)$$

$$u^{(3)} = u_M^{(3)} + \sum_{\jmath|1} \mathrm{Re}\left\{\left(\tilde{U}_{1,1;\jmath}^{(3L)}\mathcal{E}_{1;\jmath}\right)^\dagger E_{1;\jmath} + \tilde{U}_{2,0;\jmath}^{(3L)}E_{2;2\jmath}\right\} + \sum_{\jmath|2}\sum_{\ell:1}\mathrm{Re}\left\{\left(\tilde{U}_{1,1;\jmath,\ell}^{(3a)}\mathcal{E}_{1;-\jmath+\ell}\right)^\dagger E_{1;\jmath+\ell}\right.$$
$$\left. + \left(\tilde{U}_{2,0;\jmath,\ell}^{(3)}\mathcal{E}_{0;\jmath-2\ell}\right)^\dagger E_{2;\jmath} + \left(\tilde{U}_{3,1;\jmath,\ell}^{(3a)}\mathcal{E}_{1;\jmath-\ell}\right)^\dagger E_{3;\jmath+\ell}\right\} + \sum_{\jmath|3}\mathrm{Re}\,E_{1;\jmath}\left[\left(\tilde{U}_{1,1;\jmath}^{(3b)}\mathcal{E}_{1;\jmath}\right)^\dagger + \sum_{\ell:[2]}\right.$$
$$\left\{\left(\tilde{U}_{1,1;\jmath,\ell}^{(3c)}\mathcal{E}_{1;\jmath-2\ell}\right)^\dagger + \sum_{m:-1}\left(\tilde{U}_{1,1;\jmath,\ell,m}^{(3d)}\mathcal{E}_{1;-\jmath+2\ell+2m}\right)^\dagger + \sum_{m:1}\left(\left(\tilde{U}_{1,1;\jmath,\ell,m}^{(3e)}\mathcal{E}_{1;-\jmath+2m}\right)^\dagger + \left(\tilde{U}_{1,1;\jmath,\ell,m}^{(3f)}\right.\right.$$
$$\left.\left.\left.\mathcal{E}_{1;-\jmath+2\ell-2m}\right)^\dagger\right)\right\} + \sum_{\ell:[-2]}\left\{\left(\tilde{U}_{1,1;\jmath,\ell}^{(3g)}\mathcal{E}_{1;\jmath+2\ell}\right)^\dagger + \sum_{m:-1}\left(\tilde{U}_{1,1;\jmath,\ell,m}^{(3h)}\mathcal{E}_{1;-\jmath+2m}\right)^\dagger\right\}\Bigg] + \sum_{\jmath|3}\sum_{\ell:[2]}\mathrm{Re}$$
$$E_{3;\jmath}\left[\left(\tilde{U}_{3,1;\jmath,\ell}^{(3b)}\mathcal{E}_{1;-\jmath+2\ell}\right)^\dagger + \sum_{m:1}\left\{\left(\tilde{U}_{3,1;\jmath,\ell,m}^{(3c)}\mathcal{E}_{1;\jmath-2m}\right)^\dagger + \left(\tilde{U}_{3,1;\jmath,\ell,m}^{(3d)}\mathcal{E}_{1;\jmath-2\ell+2m}\right)^\dagger\right\}\right] + \ldots, \quad (6.15)$$

and

$$u^{(4)} = u_M^{(4)} + \sum_{\jmath|1}\mathrm{Re}\,\tilde{U}_{2,0;\jmath}^{(4L)}E_{2;2\jmath} + \sum_{\jmath|2}\sum_{\ell:1}\mathrm{Re}\left(\tilde{U}_{2,0;\jmath,\ell}^{(4a)}\mathcal{E}_{0;\jmath-2\ell}\right)^\dagger E_{2;\jmath} + \sum_{\jmath|3}\mathrm{Re}\left[\sum_{\ell:[2]}\left\{\left(\tilde{U}_{2,0;\jmath,\ell}^{(4b)}\right.\right.\right.$$
$$\left.\left.\left.\mathcal{E}_{0;\ell}\right)^\dagger E_{2;2\jmath-\ell} + \sum_{m:1}\left(\tilde{U}_{2,0;\jmath,\ell,m}^{(4c)}\mathcal{E}_{0;\jmath-m}\right)^\dagger E_{2;\jmath+m}\right\} + \sum_{\ell:[-2]}\left(\tilde{U}_{2,0;\jmath,\ell}^{(4d)}\mathcal{E}_{0;\ell}\right)^\dagger E_{2;2\jmath+\ell}\right] + \sum_{\jmath|4}\mathrm{Re}\,E_{2;\jmath}$$
$$\left[\sum_{\ell:2}\left\{\sum_{m:1}\left(\left(\tilde{U}_{2,0;\jmath,\ell,m}^{(4e)}\mathcal{E}_{0;\jmath-2m}\right)^\dagger + \left(\tilde{U}_{2,0;\jmath,\ell,m}^{(4f)}\mathcal{E}_{0;\jmath-2\ell+2m}\right)^\dagger\right) + \sum_{m:-1}\left(\tilde{U}_{2,0;\jmath,\ell,m}^{(4g)}\mathcal{E}_{0;\jmath-2\ell-2m}\right)^\dagger\right\}\right.$$
$$\left. + \sum_{\ell:-2}\sum_{m:-1}\left(\tilde{U}_{2,0;\jmath,\ell,m}^{(4h)}\mathcal{E}_{0;\jmath-2m}\right)^\dagger\right] + \sum_{\jmath|4}\sum_{\ell:[3]}\mathrm{Re}\,E_{2;\jmath}\left[\left(\tilde{U}_{2,0;\jmath,\ell}^{(4i)}\mathcal{E}_{0;\jmath-2\ell}\right)^\dagger + \sum_{m:[2]}\left\{\left(\tilde{U}_{2,0;\jmath,\ell,m}^{(4j)}\right.\right.\right.$$
$$\left.\left.\mathcal{E}_{0;\jmath-2\ell+2m}\right)^\dagger + \sum_{n:-1}\left(\tilde{U}_{2,0;\jmath,\ell,m,n}^{(4k)}\mathcal{E}_{0;\jmath-2m-2n}\right)^\dagger + \sum_{n:1}\left(\left(\tilde{U}_{2,0;\jmath,\ell,m,n}^{(4l)}\mathcal{E}_{0;\jmath-2n}\right)^\dagger + \left(\tilde{U}_{2,0;\jmath,\ell,m,n}^{(4m)}\right.\right.\right.$$
$$\left.\left.\left.\left.\mathcal{E}_{0;\jmath-2m+2n}\right)^\dagger\right)\right\} + \sum_{m:[-2]}\left\{\left(\tilde{U}_{2,0;\jmath,\ell,m}^{(4n)}\mathcal{E}_{0;\jmath-2\ell-2m}\right)^\dagger + \sum_{n:-1}\left(\tilde{U}_{2,0;\jmath,\ell,m,n}^{(4o)}\mathcal{E}_{0;\jmath-2n}\right)^\dagger\right\}\Bigg] + \ldots, \quad (6.16)$$

where we have put

$$E_{a;\jmath} \equiv e^{\mathrm{i}(aX-\jmath t_1)/2}, \qquad \mathcal{E}_{b;\ell} \equiv e^{\mathrm{i}(bZ+\ell z_1)}, \tag{6.17}$$

$$\left(\tilde{U}^{(k)}_{a,b;\jmath[,\ell,m,n]}\mathcal{E}_{c;\imath}\right)^{\dagger} \equiv \tilde{U}^{(k)}_{a,b;\jmath[,\ell,m,n]}\mathcal{E}_{c;\imath} + \tilde{U}^{(k)}_{a,-b;\jmath[,\ell,m,n]}\mathcal{E}_{-c;-\imath} \quad \text{for} \quad k = 2L,\ldots,4o. \tag{6.18}$$

It is easy to show that the previously defined $\tilde{E}_\jmath$, $\tilde{E}_{c\jmath}$ and $\tilde{E}_{s\jmath}$ by (5.34) are equal to $E_{2;2\jmath}$, $\frac{1}{2}E_{1;\jmath}(\mathcal{E}_{1;\jmath}+\mathcal{E}_{-1;-\jmath})$ and $-\frac{1}{2}\mathrm{i}E_{1;\jmath}(\mathcal{E}_{1;\jmath}-\mathcal{E}_{-1;-\jmath})$, respectively. The summation notations used in the above equations are defined as, for $\tilde{a} = 1, 2, 3, \ldots$,

$$\sum_{\jmath|\tilde{a}} \equiv \sum_{\jmath=-\tilde{a}J}^{\tilde{a}J}, \tag{6.19}$$

$$\sum_{\{\ell,m,n\}:\pm\tilde{a}} \equiv \sum_{\{\ell,m,n\}=\max(-\tilde{a}J,-\tilde{a}J\pm\{\jmath,\ell,m\})}^{\min(\tilde{a}J,\tilde{a}J\pm\{\jmath,\ell,m\})}, \qquad \sum_{\{\ell,m\}:[\pm\tilde{a}]} \equiv \sum_{\{\ell,m\}=\max(-\tilde{a}J,-J\pm\{\jmath,\ell\})}^{\min(\tilde{a}J,J\pm\{\jmath,\ell\})}. \tag{6.20}$$

The streamwise velocity expansions in (6.14) – (6.16) are basically composed of the Fourier components $\tilde{U}^{(k)}_{a,b;\jmath[,\ell,m,n]}E_{a;\imath}\mathcal{E}_{b;l}$ where the integers a and b are coefficients of $\frac{1}{2}\mathrm{i}X$ and $\mathrm{i}Z$ as in (6.17) and $\imath$ and l are expressed in terms of $\jmath$, ℓ, m and n. All daggered terms are composed of two components, for example, $(\tilde{U}^{(2)}_{2,0;\jmath,\ell}\mathcal{E}_{0;\jmath-2\ell})^{\dagger}E_{2;\jmath}$ in (6.14) is composed of the two components $\tilde{U}^{(2)}_{2,0;\jmath,\ell}E_{2;\jmath}\mathcal{E}_{0;\jmath-2\ell}$ and $\tilde{U}^{(2)}_{2,-0;\jmath,\ell}E_{2;\jmath}\mathcal{E}_{0;-\jmath+2\ell}$. The shape function $\tilde{U}^{(2)}_{2,-0;\jmath,\ell}$ is different from $\tilde{U}^{(2)}_{2,0;\jmath,\ell}$ in general, although they will be shown to be the same in the present case by (6.26). By putting $J = 0$, or consequently $\jmath = \ell = m = n = 0$, we can recover the expansions for the single resonant-triad case given by Goldstein & Lee (1992), Wu (1992) and Lee (1997a). The oblique-mode velocity jump across the critical layer can be obtained from those of the nine Fourier components given in (6.15) with the subscript $1,1;\jmath[,\ell,m]$ and the superscripts $3L$, $3a$, …, $3h$. Meanwhile, we need to consider all sixteen components in (6.16), denoted with the superscripts $4L$, $4a$, …, $4o$, in order to obtain the velocity jump of the plane wave.

The solution of the critical-layer equation for the $\tilde{U}^{(2)}_{0,2;j,\ell}E_{0;j}\mathcal{E}_{2;j+2\ell}$ component, given in Part 2, shows that the nonlinear interaction within the critical layer produces a non-zero jump of this component (Goldstein & Choi 1989). It is worth to note that this term is a function of the slow time t_1 defined by (5.24). For the single-resonant-triad interaction, the subscripts j and ℓ become zero and thus this component becomes steady as we expected from the results of Goldstein & Choi (1989), Goldstein & Lee (1992, 1993) and Wu (1992).

By substituting (6.1) into the base mean-flow component in (5.30), or directly into (3.13) to (3.16), re-expanding the result and comparing with (6.6), we can show that $u^{(2)}_M$ and $u^{(3)}_M$ in (6.14) and (6.15) are given by

$$u^{(2)}_M = a^{(2)}_{1M}\bar{\eta}^2 + a^{(2)}_{2M}\bar{\eta} + a^{(2)}_{3M}x_1 + \ldots, \tag{6.21}$$

$$u^{(3)}_M = a^{(3)}_{1M}\bar{\eta}^3 + a^{(3)}_{2M}\bar{\eta}^2 + a^{(3)}_{3M}\bar{\eta}x_1 + \ldots, \tag{6.22}$$

where

$$a^{(2)}_{1M} = \tfrac{1}{2}\bar{\mu}_c + \ldots, \tag{6.23}$$

and $\bar{\mu}_c$ is given by (3.19). The constant $a^{(2)}_{1M}$ is nearly equal to one half of the double derivative of the base mean flow at the critical level $y = \sigma Y_c$ divided by the scaling factor σ^{r-1}. The other constants $a^{(2)}_{2M}$, $a^{(2)}_{3M}$, $a^{(3)}_{1M}$, $a^{(3)}_{2M}$ and $a^{(3)}_{3M}$ can also be found although the results were not presented since they do not play any major role in the analysis. The last terms in (6.21) and (6.22) are functions of x_1 and they are included in order to match the slight viscous correction that enters the external solution due to the slow viscous spreading of the mean flow as in (3.13).

The expansions for the other velocities $\bar{v}^{(k)}$ and $w^{(k)}$ and the pressure $p^{(k)}$ for k =2, 3 and 4 can be obtained if we replace $\tilde{U}^{(l)}_{a,b;j[,\ell,m,n]}$ in (6.14) to (6.16) by $\tilde{V}^{(l)}_{a,b;j[,\ell,m,n]}$, $\tilde{W}^{(l)}_{a,b;j[,\ell,m,n]}$

and $\tilde{P}^{(l)}_{a,b;\jmath[,\ell,m,n]}$ and also replace the mean flow component $u^{(k)}_M$ by $\bar{v}^{(k)}_M$, $w^{(k)}_M$ and $p^{(k)}_M$, respectively. The mean velocity components $\bar{v}^{(k)}_M$ and $w^{(k)}_M$ can be found by matching (6.7) and (6.8) with the outer solutions (3.2) and (3.3) as

$$\bar{v}^{(2)}_M = b^{(2)}_M, \quad \bar{v}^{(3)}_M = b^{(3)}_{1M}\bar{\eta} + \ldots, \quad w^{(2)}_M = w^{(3)}_M = 0, \tag{6.24}$$

where $b^{(2)}_M$ and $b^{(3)}_{1M}$ are constants. The transverse velocity components $\bar{v}^{(2)}_M$ and $\bar{v}^{(3)}_M$ are non-zero because of the viscous spreading of the mean flow as mentioned in §3. The nonlinearly-generated $Z-$independent components of the spanwise velocity , $\tilde{W}^{(l)}_{2,0;\jmath[,\ell,m,n]}$, are not zero inside the critical layer although they vanish on its edge.

If we substitute the expansions (6.10), (6.14) – (6.16) for $u^{(k)}$, (6.11) for $w^{(1)}$ and similar expansions for $\bar{v}^{(k)}$, $w^{(k)}$ and $p^{(k)}$ along with the mean-flow components (6.12), (6.21), (6.22) and (6.24) into the nonlinear equations in Appendix A and if we use the relation

$$\sum_{\jmath|\tilde{a}} F_\jmath \sum_{\ell|\tilde{b}} G_\ell = \sum_{\jmath|\tilde{a}+\tilde{b}} \sum_{\ell=\max\left(-\tilde{b}J,-\tilde{a}J\pm\jmath\right)}^{\min\left(\tilde{b}J,\tilde{a}J\pm\jmath\right)} F_{\jmath\mp\ell} G_\ell, \tag{6.25}$$

where the summation notation defined by (6.19) is used and $\tilde{a}$ and $\tilde{b}$ are positive integers, then we can obtain a system of partial differential critical-layer equations, which will be shown in the following section, after considerable manipulation. The equations were given in Goldstein & Lee (1992) and Lee (1997a) for the single-resonant-triad interaction. The system of critical-layer equations can be solved analytically (Goldstein & Choi 1989; Goldstein & Lee 1992, 1993; Wu 1992, 1995; Wu *et al.* 1993) or numerically (Lee 1997a) with the transverse boundary conditions at $\bar{\eta} = \pm\infty$ that can be found from the matching with the outer solutions (5.30) to (5.33).

The outer solutions (5.30) to (5.33) are obtained for the case when the oblique-mode amplitudes with positive and negative propagation angles are the same. We can show from

the critical-layer equations and their boundary conditions that

$$\left\{\tilde{U},\tilde{V},\tilde{W},\tilde{P}\right\}^{(k)}_{a,b;\jmath[,\ell,m,n]} = \left\{\tilde{U},\tilde{V},-\tilde{W},\tilde{P}\right\}^{(k)}_{a,-b;\jmath[,\ell,m,n]} \tag{6.26}$$

for all daggered components, i.e. $()^{\dagger}$, that appear in the expansions (6.14) to (6.16) and

$$\left\{\tilde{U},\tilde{V},\tilde{W},\tilde{P}\right\}^{(2)}_{0,2;\jmath,\ell} = \left\{\tilde{U},\tilde{V},-\tilde{W},\tilde{P}\right\}^{(2)^*}_{-0,2;\jmath\ell}, \tag{6.27}$$

where the asterisk denotes the complex conjugate.

The solutions of the critical-layer equations have to match onto the discontinuous $O(\delta_{3d}\sigma^r) = O(\sigma^{4r+1})$ and $O(\epsilon_{2d}\sigma^r) = O(\sigma^{5r+1})$ terms in (5.30) and also $O(\delta_{3d}\sigma^{r+2})$ and $O(\epsilon_{2d}\sigma^{r+2})$ terms in (5.31) for the oblique and two-dimensional modes, respectively. It follows from (5.30), (5.31), (6.6) and (6.7) along with (6.1) and (6.5) that

$$\int_{-\infty}^{\infty} \bar{v}^{(3)}_{\bar{\eta}\bar{\eta}} d\bar{\eta} = -\tfrac{1}{2}\mathrm{i}\bar{\alpha}\int_{-\infty}^{\infty} u^{(3)}_{\bar{\eta}} d\bar{\eta} = \sum_{\jmath=-J}^{J} \mathrm{Re}\, 2\bar{\mu}_c\bar{\gamma}Y_c\left(\phi^+_\jmath - \phi^-_\jmath\right)\bar{A}_\jmath\tilde{E}_{c\jmath} + \ldots, \tag{6.28}$$

$$\int_{-\infty}^{\infty} \bar{v}^{(4)}_{\bar{\eta}\bar{\eta}} d\bar{\eta} = -\mathrm{i}\bar{\alpha}\int_{-\infty}^{\infty} u^{(4)}_{\bar{\eta}} d\bar{\eta} = \sum_{\jmath=-J}^{J} \mathrm{Re}\,\bar{\mu}_c\bar{\alpha}Y_c\left(\ddot{\phi}^+_\jmath - \ddot{\phi}^-_\jmath\right)\bar{B}_\jmath\tilde{E}_\jmath + \ldots, \tag{6.29}$$

where $\tilde{E}_\jmath$ and $\tilde{E}_{c\jmath}$ are defined in (5.34). The phase jumps in (6.28) and (6.29) can be eliminated by using (5.27) and (5.28) to show that

$$\int_{-\infty}^{\infty} \bar{v}^{(3)}_{\bar{\eta}\bar{\eta}} d\bar{\eta} = \sum_{\jmath=-J}^{J} \mathrm{Re}\,\frac{2\tau_w\bar{c}^2}{\bar{\gamma}Y_c}\left[\left(\cos\theta + \frac{1}{\cos\theta}\right)\left(\bar{A}'_\jmath - \frac{\mathrm{i}}{4}\jmath\tilde{\chi}\bar{\alpha}\bar{A}_\jmath\right) - \frac{\bar{\gamma}^2}{\bar{c}^2}\left(\frac{\sigma^r\lambda}{\bar{s}}\right)^{1/2}\bar{A}_\jmath\right]\tilde{E}_{c\jmath}, \tag{6.30}$$

$$\int_{-\infty}^{\infty} u^{(4)}_{\bar{\eta}} d\bar{\eta} = \sum_{\jmath=-J}^{J} \mathrm{Re}\,\frac{2\mathrm{i}\tau_w\bar{c}^2}{\bar{\alpha}^2 Y_c}\left[\bar{B}'_\jmath - \left\{\frac{\mathrm{i}}{2}\jmath\tilde{\chi}\bar{\alpha} + \frac{\bar{\alpha}^2}{2\bar{c}^2}\left(\frac{\sigma^r\lambda}{2\bar{s}}\right)^{1/2}\right\}\bar{B}_\jmath\right]\tilde{E}_\jmath. \tag{6.31}$$

From the expansion for $\bar{v}^{(3)}$ that is similar to (6.15) and the expansion (6.16) for $u^{(4)}$ along with (6.26) we can show that

$$\bar{v}^{(3)} = \sum_{\jmath=-J}^{J} \mathrm{Re}\, 2\tilde{E}_{c\jmath}\left[\tilde{V}^{(3L)}_{1,1;\jmath} + \tilde{V}^{(3a)}_{1,1;0,\jmath} + \tilde{V}^{(3b)}_{1,1;\jmath} + \tilde{V}^{(3c)}_{1,1;\jmath,0} + \tilde{V}^{(3g)}_{1,1;\jmath,0} + \sum_{\ell=-J+\jmath}^{J+\jmath}\left(\tilde{V}^{(3d)}_{1,1;\jmath,\ell,\jmath-\ell}\right.\right.$$
$$\left.\left. + \tilde{V}^{(3e)}_{1,1;\jmath,\ell,\jmath} + \tilde{V}^{(3f)}_{1,1;\jmath,\ell,\ell-\jmath}\right) + \sum_{\ell=-J-\jmath}^{J-\jmath} \tilde{V}^{(3h)}_{1,1;\jmath,\ell,\jmath}\right] + \ldots, \tag{6.32}$$

$$u^{(4)} = \sum_{\jmath=-J}^{J} \mathrm{Re}2\tilde{E}_\jmath \left[\tfrac{1}{2}\tilde{U}^{(4L)}_{2,0;\jmath} + \tilde{U}^{(4a)}_{2,0;2\jmath,\jmath} + \tilde{U}^{(4b)}_{2,0;\jmath,0} + \tilde{U}^{(4d)}_{2,0;\jmath,0} + \tilde{U}^{(4i)}_{2,0;2\jmath,\jmath} + \sum_{\ell=-J+\jmath}^{J+\jmath} \left(\tilde{U}^{(4c)}_{2,0;\jmath,\ell,\jmath} \right.\right.$$
$$\left. + \tilde{U}^{(4e)}_{2,0;2\jmath,\ell,\jmath} + \tilde{U}^{(4f)}_{2,0;2\jmath,\ell,\ell-\jmath} + \tilde{U}^{(4g)}_{2,0;2\jmath,\ell,\jmath-\ell} \right) + \sum_{\ell=-J-\jmath}^{J-\jmath} \tilde{U}^{(4h)}_{2,0;2\jmath,\ell,\jmath} + \sum_{\ell=-J+2\jmath}^{J+2\jmath} \left\{ \tilde{U}^{(4j)}_{2,0;2\jmath,\ell,\ell-\jmath} \right.$$
$$+ \tilde{U}^{(4n)}_{2,0;2\jmath,\ell,\jmath-\ell} + \sum_{m=\max(-J+\jmath,-J+\ell)}^{\min(J+\jmath,J+\ell)} \left(\tilde{U}^{(4k)}_{2,0;2\jmath,\ell,m,\jmath-m} + \tilde{U}^{(4l)}_{2,0;2\jmath,\ell,m,\jmath} + \tilde{U}^{(4m)}_{2,0;2\jmath,\ell,m,m-\jmath} \right)$$
$$\left.\left. + \sum_{m=\max(-J-\jmath,-J-\ell)}^{\min(J-\jmath,J-\ell)} \tilde{U}^{(4o)}_{2,0;2\jmath,\ell,m,\jmath} \right\} \right] + \ldots, \qquad (6.33)$$

where we have only shown the components of the base subharmonic and fundamental frequencies. Substituting the above equations into (6.30) and (6.31) and by equating the coefficients of $\tilde{E}_{c\jmath}$ and $\tilde{E}_\jmath$ for the oblique and plane waves, respectively, we obtain the jump equations that will be given in the following section. They arise from the requirement that the velocity jumps across the critical layer which are calculated from the internal critical-layer solutions are equal to those calculated from the external solutions. The jump equations must be solved with the system of critical-layer equations to determine the unknown instability wave amplitudes $\bar{A}_\jmath$ and $\bar{B}_\jmath$.

7. The system of critical-layer equations and the jump equations

In this section we will present the system of partial differential critical-layer equations along with the transverse boundary conditions and the jump equations. These final equations are normalized in such a way that their nonlinear growth parts are free from the mean flow dependent parameters (Lee 1997a).

It is convenient to introduce the following normalized variables (Goldstein & Lee 1992;

Lee 1997a)

$$\bar{x} = \hat{\kappa}\left(\tfrac{1}{2}\tau_w\bar{\alpha}x_1 - x_o\right), \quad \eta = \bar{\eta}/(\hat{\kappa}\bar{c}) - \tfrac{1}{2}\eta_o, \quad \tilde{X} = X - X_o, \tag{7.1}$$

$$\bar{\lambda} = \frac{2\lambda}{\hat{\kappa}^3\tau_w\bar{\alpha}\bar{c}^3}, \quad \{\bar{\chi},\hat{\chi}\} = \frac{1}{\hat{\kappa}\tau_w}\{\chi,\tilde{\chi}\}, \tag{7.2}$$

and

$$\bar{a}_{1M}^{(2)} = \frac{2\pi Y_c\bar{\alpha}}{\hat{\kappa}\tau_w^3\bar{c}}a_{1M}^{(2)} = \frac{\pi Y_c\bar{\alpha}}{\hat{\kappa}\tau_w^3\bar{c}}\bar{\mu}_c, \tag{7.3}$$

where the positive real constant $\hat{\kappa}$ is a normalization parameter which can be chosen arbitrarily, x_o, η_o and X_0 are coordinate origin shifts to be chosen subsequently, x_1, X, λ and $\bar{\eta}$ are defined by (2.3), (3.5), (2.8) and (6.1), τ_w is given by (3.15) or (3.16) and $\tilde{\chi}$ is given by (5.23). The frequency-detuning factor χ, introduced by (2.6), can be given as an input for a problem. The mean flow coefficient $a_{1M}^{(2)}$ was defined by (6.21) and (6.23). As in before the subscript 0 has been omitted for the quantities of the 0th resonant-triad ($\jmath = 0$).

Following Lee (1997a) the dependent variables are normalized as, for $-J \leqslant \jmath \leqslant J$,

$$A_\jmath \equiv \frac{(Y_cM)^{1/2}}{\hat{\kappa}^3\bar{c}}\mathcal{D}_{1;\jmath}\bar{A}_\jmath, \quad B_\jmath \equiv \frac{M}{\hat{\kappa}^4}\mathcal{D}_{2;2\jmath}\bar{B}_\jmath, \quad Q_\jmath^{(1)} = \frac{(Y_cM)^{1/2}}{\hat{\kappa}^2\bar{c}\sin\theta}\mathcal{D}_{1;\jmath}\tilde{Q}_\jmath^{(1)}, \tag{7.4}$$

where $\bar{A}_\jmath$ and $\bar{B}_\jmath$ are related to $\tilde{A}_\jmath$ and $\tilde{B}_\jmath$ in (3.1) to (3.4) by (5.26), $\tilde{Q}_\jmath^{(1)}$ is the mode shape of the leading-order solution given by (6.10) and (6.11), θ defined in (5.29) is $\pi/3$ at the leading order and we have put

$$M \equiv 8\pi Y_c\bar{\beta}^2/(\tau_w^3\bar{\alpha}\bar{c}^3), \tag{7.5}$$

$$\mathcal{D}_{a;\jmath}(\bar{x}) \equiv \exp\left[\tfrac{1}{2}\mathrm{i}a\,(X_o + \eta_o\bar{x}) - \mathrm{i}\jmath\bar{\chi}\bar{x}\right]. \tag{7.6}$$

The other normalized variables $\{U,V,W,P\}_{a,b;\jmath[,\ell,m,n]}^{(k)}$ of $\{\tilde{U},\tilde{V},\tilde{W},\tilde{P}\}_{a,b;\jmath[,\ell,m,n]}^{(k)}$, which are coefficients of the Fourier series given in (6.14) to (6.16) and similar ones for the transverse and spanwise velocities and pressure, are defined in Appendix B for $k = 2$, 3 and 4.

If we put

$$\mathcal{L}_n \equiv \frac{\partial}{\partial \bar{x}} + in\eta - \bar{\lambda}\frac{\partial^2}{\partial \eta^2}, \tag{7.7}$$

the leading-order equation of the system of critical-layer equations becomes

$$\mathcal{L}_1 Q_j^{(1)} = A_j, \tag{7.8}$$

which can be solved with the transverse boundary condition

$$Q_j^{(1)} \to 0 \quad \text{as} \quad \eta \to \pm\infty. \tag{7.9}$$

The second-order equations are

$$\mathcal{L}_0 W_{0,0;j}^{(2)} = -\tfrac{1}{2}\sum_{\ell:-1} A_{j+\ell} Q_{\ell\eta}^{(1)^*}, \quad U_{0,0;j}^{(2)} = -W_{0,0;j}^{(2)}, \quad V_{0,0;j}^{(2)} = 0, \tag{7.10}$$

$$\mathcal{L}_0 W_{0,2;j,\ell}^{(2)} = F_{(1)|j+\ell} Q_\ell^{(1)^*}, \; \mathcal{L}_0 U_{0,2;j,\ell\eta}^{(2)} = 2\mathrm{i} W_{0,2;j,\ell}^{(2)} + \left(\mathcal{L}_0 W_{0,2;j,\ell}^{(2)}\right)_\eta, \; V_{0,2;j,\ell\eta}^{(2)} = 2W_{0,2;j,\ell}^{(2)}, \tag{7.11}$$

$$\mathcal{L}_1 W_{1,1;j}^{(2L)} = -P_{1,1;j}^{(2L)} - \mathcal{L}_1 W_{1,1;j}^{(2M)}, \quad V_{1,1;j}^{(2L)} = \left(\eta + \tfrac{1}{2}\eta_o\right) A_j + \bar{v}_{1,1;j}^{(2L)}(\bar{x}),$$

$$U_{1,1;j}^{(2L)} = -W_{1,1;j}^{(2L)} - (\sin^2\theta)\left[Q_{j\bar{x}}^{(1)} + \mathrm{i}(j\bar{\chi} - \tfrac{1}{2}\eta_o) Q_j^{(1)}\right] + \tfrac{\sqrt{3}}{4}\mathrm{i}j(\sin 2\theta)\hat{\chi} Q_j^{(1)} + A_j, \tag{7.12}$$

$$V_{2,0;j}^{(2L)} = B_j, \quad U_{2,0;j}^{(2L)} = W_{2,0;j}^{(2L)} = 0 \tag{7.13}$$

$$\mathcal{L}_2 W_{2,0;j,\ell}^{(2)} = -F_{(-1)|j-\ell} Q_\ell^{(1)}, \quad \mathcal{L}_2 U_{2,0;j,\ell\eta}^{(2)} = \left(\mathcal{L}_2 W_{2,0;j,\ell}^{(2)}\right)_\eta, \quad V_{2,0;j,\ell\eta}^{(2)} = 2U_{2,0;j,\ell}^{(2)}, \tag{7.14}$$

$$\mathcal{L}_2 W_{2,2;j}^{(2)} = \tfrac{1}{2}\sum_{\ell:1} A_{j-\ell} Q_{\ell\eta}^{(1)}, \quad U_{2,2;j}^{(2)} = -W_{2,2;j}^{(2)}, \quad V_{2,2;j}^{(2)} = 0, \tag{7.15}$$

and

$$P_{1,1;j\eta}^{(2L)} = P_{2,0;j\eta}^{(2L)} = 0, \quad P_{a,b;j[,\ell]\eta}^{(2)} = 0, \tag{7.16}$$

where the summation notation is defined in (6.20), $W_{1,1;j}^{(2M)}$ is given in Appendix C and $\bar{v}_{1,1;j}^{(2L)}(\bar{x})$ could be found, although the present analysis does not require that, by matching

with the outer solution (3.2), (5.2), (5.31), (6.1), (6.5) and (6.7). The subscript η denotes the differentiation with respect to η, i.e. $\partial/\partial\eta$, as usual, and the subscript $\{a,b\}$ in (7.16) denotes either $\{0,0\}$, $\{0,2\}$, $\{2,0\}$ or $\{2,2\}$. We have also put

$$F_{(d)|J} \equiv \tfrac{1}{2}A_J\tfrac{\partial}{\partial\eta} + \mathrm{i}d\tau(\sin^2\theta)Q_J^{(1)} \quad \text{for} \quad d = 0, \pm1, \pm2, \ldots, \tag{7.17}$$

and

$$\tau \equiv \bar{c}/(\tau_w Y_c), \tag{7.18}$$

where τ becomes unity at the leading-order if we use (3.20). Some of the simple equations have been solved with appropriate transverse boundary conditions and we have also used, in (7.11) and (7.15), the solutions of (7.16),

$$P^{(2)}_{0,2;J,\ell} = P^{(2)}_{2,2;J} = 0. \tag{7.19}$$

From (3.4), (3.11), (5.2), (5.33) and (6.9), we can find $P^{(2L)}_{1,1;J}(\bar{x})$, but it does not play any major role in computing the amplitudes A_J and B_J.

The transverse boundary conditions are

$$W^{(2L)}_{1,1;J}, W^{(2)}_{a,b;J[,\ell]}, U^{(2)}_{0,2;J,\ell\eta}, U^{(2)}_{2,0;J,\ell\eta} \to 0 \quad \text{as} \quad \eta \to \pm\infty. \tag{7.20}$$

The solutions of (7.11) given in Part 2 show that $U^{(2)}_{0,2;J,\ell}(\eta=\infty) - U^{(2)}_{0,2;J,\ell}(\eta=-\infty)$ and $V^{(2)}_{0,2;J,\ell}(\eta=\infty) - V^{(2)}_{0,2;J,\ell}(\eta=-\infty)$ are non-zero, therefore,

$$U^{(2)}_{0,2;J,\ell} \to \bar{U}^{(2)\pm\infty}_{0,2;J,\ell}, \quad V^{(2)}_{0,2;J,\ell} \to \bar{V}^{(2)\pm\infty}_{0,2;J,\ell} \quad \text{as} \quad \eta \to \pm\infty, \tag{7.21}$$

where $\bar{U}^{(2)\pm\infty}_{0,2;J,\ell}$ and $\bar{V}^{(2)\pm\infty}_{0,2;J,\ell}$ are functions of $\bar{x}$.

The velocity jump across the critical layer for the oblique mode will be obtained by solving the following third-order equations

$$\mathcal{L}_1 W^{(3L)}_{1,1;J} = -P^{(3L)}_{1,1;J} - \mathcal{L}_1 W^{(3M)}_{1,1;J}, \quad \mathcal{L}_1 V^{(3L)}_{1,1;J\eta\eta} = 2\mathrm{i}\bar{a}^{(2)}_{1M} A_J, \tag{7.22}$$

$$\left\{\mathcal{L}_1 W^{(3a)}_{1,1;\jmath,\ell}, \mathcal{L}_1 V^{(3a)}_{1,1;\jmath,\ell\eta\eta}\right\} = -\left\{P^{(3a)}_{1,1;\jmath,\ell}, 0\right\} + \left\{1, 2\tfrac{\partial}{\partial\eta}\right\}(\cos^2\theta) Q^{(1)^*}_{(-\jmath+\ell)\eta} V^{(2L)}_{2,0;\ell}, \tag{7.23}$$

$$\mathcal{L}_1 W^{(3b)}_{1,1;\jmath} = -P^{(3b)}_{1,1;\jmath} + \tfrac{\mathrm{i}}{2}\left[\sum_{\ell:[2]}\left(A_{\jmath-\ell} W^{(2)}_{0,0;\ell\eta} - A^*_{(-\jmath+\ell)} W^{(2)}_{2,2;\ell\eta}\right) + \sum_{\ell:[-2]} A_{\jmath+\ell} W^{(2)^*}_{0,0;\ell\eta}\right], \; V^{(3b)}_{1,1;\jmath} = 0, \tag{7.24}$$

$$\mathcal{L}_1 W^{(3c)}_{1,1;\jmath,\ell} = -P^{(3c)}_{1,1;\jmath,\ell} - \mathrm{i}F_{(1)|\jmath-\ell} W^{(2)}_{0,0;\ell}, \quad \mathcal{L}_1 V^{(3c)}_{1,1;\jmath,\ell\eta\eta} = \mathrm{i}A_{\jmath-\ell} U^{(2)}_{0,0;\ell\eta\eta}, \tag{7.25}$$

$$\mathcal{L}_1 W^{(3d)}_{1,1;\jmath,\ell,m} = -P^{(3d)}_{1,1;\jmath,\ell,m} + G^{(2|0,1:1,1,1)}_{(\jmath-\ell)|0,2;\ell,m}, \quad \mathcal{L}_1 V^{(3d)}_{1,1;\jmath,\ell,m\eta\eta} = \left[G^{(2|1,1:2,2,0)}_{(\jmath-\ell)|0,2;\ell,m}\right]_\eta, \tag{7.26}$$

$$\mathcal{L}_1 W^{(3e)}_{1,1;\jmath,\ell,m} = -P^{(3e)}_{1,1;\jmath,\ell,m} + \tilde{G}^{(2|0,1:-1,-1,-3)}_{(-\jmath+\ell)|2,0;\ell,m}, \quad \mathcal{L}_1 V^{(3e)}_{1,1;\jmath,\ell,m\eta\eta} = -\left[\tilde{G}^{(2|1,-1:2,0,-2)}_{(-\jmath+\ell)|2,0;\ell,m}\right]_\eta, \tag{7.27}$$

$$\mathcal{L}_1 W^{(3f)}_{1,1;\jmath,\ell,m} = -P^{(3f)}_{1,1;\jmath,\ell,m} - \tilde{G}^{(2|0,1:1,-1,3)}_{(-\jmath+\ell)|2,0;\ell,m}, \quad \mathcal{L}_1 V^{(3f)}_{1,1;\jmath,\ell,m\eta\eta} = -\left[\tilde{G}^{(2|1,1:2,0,2)}_{(-\jmath+\ell)|2,0;\ell,m}\right]_\eta, \tag{7.28}$$

$$\mathcal{L}_1 W^{(3g)}_{1,1;\jmath,\ell} = -P^{(3g)}_{1,1;\jmath,\ell} - \mathrm{i}F_{(1)|\jmath+\ell} W^{(2)^*}_{0,0;\ell}, \quad \mathcal{L}_1 V^{(3g)}_{1,1;\jmath,\ell\eta\eta} = \mathrm{i}A_{\jmath+\ell} U^{(2)^*}_{0,0;\ell\eta\eta}, \tag{7.29}$$

$$\mathcal{L}_1 W^{(3h)}_{1,1;\jmath,\ell,m} = -P^{(3h)}_{1,1;\jmath,\ell,m} + \tilde{G}^{(2|0,1:-1,-1,1)^*}_{(\jmath+\ell)|0,2;\ell,m}, \quad \mathcal{L}_1 V^{(3h)}_{1,1;\jmath,\ell,m\eta\eta} = -\left[\tilde{G}^{(2|1,-1:2,-2,0)^*}_{(\jmath+\ell)|0,2;\ell,m}\right]_\eta, \tag{7.30}$$

with

$$U^{(k)}_{1,1;\jmath[,\ell,m]} = V^{(k)}_{1,1;\jmath[,\ell,m]\eta} - W^{(k)}_{1,1;\jmath[,\ell,m]} + \mathcal{R}^{(k)}_{1,1;\jmath[,\ell,m]} \quad \text{for} \quad k = 3L, 3a, \ldots, 3h, \tag{7.31}$$

and

$$P^{(k)}_{1,1;\jmath[,\ell,m]\eta} = 0 \quad \text{for} \quad k = 3L, 3a, \ldots, 3h, \tag{7.32}$$

where $\mathcal{R}^{(k)}_{1,1;\jmath[,\ell,m]}$ in (7.31) is equal to zero if $k \neq 3L$ and $\mathcal{R}^{(3L)}_{1,1;\jmath}$ is given in Appendix C along with $W^{(3M)}_{1,1;\jmath}$ in (7.22), We have put, in addition to (5.29), (6.20), (7.3), (7.17) and (7.18), that

$$\left\{G, \tilde{G}\right\}^{(k|d_1,d_2:d_3,d_4,d_5)}_{(\jmath)|a,b;\ell[,m,n]} \equiv \tfrac{\mathrm{i}}{2}\left(d_1 U^{(k)}_{a,b;\ell[,m,n]} + d_2 W^{(k)}_{a,b;\ell[,m,n]}\right)_\eta \left\{A_\jmath, A^*_\jmath\right\}$$
$$+ d_3 \tfrac{\tau}{2}(\sin^2\theta)\left(d_4 U^{(k)}_{a,b;\ell[,m,n]} + d_5 W^{(k)}_{a,b;\ell[,m,n]} - V^{(k)}_{a,b;\ell[,m,n]}\tfrac{\partial}{\partial\eta}\right)\left\{Q^{(1)}_\jmath, Q^{(1)^*}_\jmath\right\}, \tag{7.33}$$

where d_1 to d_5 are real constants. The pressure $P^{(k)}_{1,1;\jmath[,\ell,m]}(\bar{x})$ for $k = 3L,\ 3a,\ \ldots,\ 3h$ could be found by matching with the outer solution, but it is unnecessary in this analysis.

The above partial differential equations can be solved subject to the transverse boundary conditions

$$(W^{(3L)}_{1,1;\jmath} + W^{(3M)}_{1,1;\jmath}), W^{(k)}_{1,1;\jmath[,\ell,m]}, V^{(3L)}_{1,1;\jmath\eta\eta}, V^{(k)}_{1,1;\jmath[,\ell,m]\eta\eta} \to 0 \quad \text{as} \quad \eta \to \pm\infty, \tag{7.34}$$

for $k = 3a,\ 3b,\ \ldots,\ 3h$.

The other third-order equations that must be solved in order to compute the velocity jump of the plane wave across the critical layer are

$$U^{(3L)}_{2,0;\jmath} = B_\jmath, \quad V^{(3L)}_{2,0;\jmath} = 2\left(\eta + \tfrac{1}{2}\eta_o\right) B_\jmath + \bar{v}^{(3L)}_{2,0;\jmath}(\bar{x}), \quad W^{(3L)}_{2,0;\jmath} = 0, \tag{7.35}$$

$$\mathcal{L}_2 W^{(3)}_{2,0;\jmath,\ell} = \mathcal{Z}^{(3)}_{2,0;\jmath,\ell}, \quad \mathcal{L}_2 U^{(3)}_{2,0;\jmath,\ell\eta} = \mathcal{R}^{(3)}_{2,0;\jmath,\ell}, \quad V^{(3)}_{2,0;\jmath,\ell\eta} = 2U^{(3)}_{2,0;\jmath,\ell} + \mathcal{Y}^{(3)}_{2,0;\jmath,\ell}, \tag{7.36}$$

$$\mathcal{L}_3 \left\{W^{(3a)}_{3,1;\jmath,\ell}, V^{(3a)}_{3,1;\jmath,\ell\eta\eta}\right\} = -\left\{P^{(3a)}_{3,1;\jmath,\ell}, 0\right\} + (\cos^2\theta) V^{(2L)}_{2,0;\ell} \left\{\tfrac{\partial}{\partial\eta}, -2\tfrac{\partial^2}{\partial\eta^2}\right\} Q^{(1)}_{(\jmath-\ell)}, \tag{7.37}$$

$$\mathcal{L}_3 W^{(3b)}_{3,1;\jmath,\ell} = -P^{(3b)}_{3,1;\jmath,\ell} + \mathrm{i}F_{(-1)|\jmath-\ell} W^{(2)}_{2,2;\ell}, \quad \mathcal{L}_3 V^{(3b)}_{3,1;\jmath,\ell\eta\eta} = -2\mathrm{i}\left[F_{(-4)|\jmath-\ell} W^{(2)}_{2,2;\ell}\right]_\eta, \tag{7.38}$$

$$\mathcal{L}_3 W^{(3c)}_{3,1;\jmath,\ell,m} = -P^{(3c)}_{3,1;\jmath,\ell,m} + G^{(2|0,1:-1,1,-1)}_{(\jmath-\ell)|2,0;\ell,m}, \quad \mathcal{L}_3 V^{(3c)}_{3,1;\jmath,\ell,m\eta\eta} = \left[G^{(2|3,1:2,4,2)}_{(\jmath-\ell)|2,0;\ell,m}\right]_\eta, \tag{7.39}$$

$$\mathcal{L}_3 W^{(3d)}_{3,1;\jmath,\ell,m} = -P^{(3d)}_{3,1;\jmath,\ell,m} - G^{(2|0,1:1,1,1)}_{(\jmath-\ell)|2,0;\ell,m}, \quad \mathcal{L}_3 V^{(3d)}_{3,1;\jmath,\ell,m\eta\eta} = \left[G^{(2|3,-1:2,4,-2)}_{(\jmath-\ell)|2,0;\ell,m}\right]_\eta, \tag{7.40}$$

with

$$U^{(k)}_{3,1;\jmath,\ell[,m]} = \tfrac{1}{3}\left(V^{(k)}_{3,1;\jmath,\ell[,m]\eta} - W^{(k)}_{3,1;\jmath,\ell[,m]}\right) \quad \text{for} \quad k = 3a, 3b, 3c, 3d, \tag{7.41}$$

and

$$P^{(3L)}_{2,0;\jmath\eta} = P^{(3)}_{2,0;\jmath,\ell\eta} = 0, \quad P^{(k)}_{3,1;\jmath,\ell[,m]\eta} = 0 \quad \text{for} \quad k = 3a, 3b, 3c, 3d, \tag{7.42}$$

where we have used (5.29), (7.17) and (7.33), $\mathcal{Z}^{(3)}_{2,0;\jmath,\ell}$, $\mathcal{R}^{(3)}_{2,0;\jmath,\ell}$ and $\mathcal{Y}^{(3)}_{2,0;\jmath,\ell}$ in (7.36) are given in Appendix C and $\bar{v}^{(3L)}_{2,0;\jmath}(\bar{x})$ can be found from (3.2), (5.2), (5.31), (6.1), (6.5) and (6.7) although we do not need to obtain it.

The transverse boundary conditions are

$$W^{(3)}_{2,0;\jmath,\ell}, U^{(3)}_{2,0;\jmath,\ell\eta}, W^{(k)}_{3,1;\jmath,\ell[,m]}, V^{(k)}_{3,1;\jmath,\ell[,m]\eta\eta} \to 0 \quad \text{as} \quad \eta \to \pm\infty, \tag{7.43}$$

for $k = 3a$, $3b$, $3c$ and $3d$.

Finally, the velocity jump across the critical layer for the two-dimensional instability wave can be found by solving the following fourth-order equations:

$$\mathcal{L}_2 U^{(4L)}_{2,0;\jmath\eta} = 4\mathrm{i}\bar{a}^{(2)}_{1M} B_\jmath, \tag{7.44}$$

$$\mathcal{L}_2 U^{(4a)}_{2,0;\jmath,\ell\eta} = \mathcal{R}^{(4a)}_{2,0;\jmath,\ell}, \quad \mathcal{L}_2 U^{(4b)}_{2,0;\jmath,\ell\eta} = \mathrm{i}V^{(2L)}_{2,0;\jmath-\ell} U^{(2)}_{0,0;\ell\eta\eta}, \quad \mathcal{L}_2 U^{(4d)}_{2,0;\jmath,\ell\eta} = \mathrm{i}V^{(2L)}_{2,0;\jmath+\ell} U^{(2)^*}_{0,0;\ell\eta\eta}, \tag{7.45}$$

$$\mathcal{L}_2 U^{(4e)}_{2,0;\jmath,\ell,m\eta} = \mathcal{L}_2 U^{(4f)}_{2,0;\jmath,\ell,m\eta} = -\mathrm{i}\tau(\tan^2\theta)\left(U^{(2)}_{2,0;\ell,m\eta} - \tfrac{1}{2}V^{(2)}_{2,0;\ell,m}\tfrac{\partial^2}{\partial\eta^2}\right)\left(U^{(2)}_{0,0;\jmath-\ell} + U^{(2)^*}_{0,0;(-\jmath+\ell)}\right), \tag{7.46}$$

$$\mathcal{L}_2\left\{U^{(4g)}_{2,0;\jmath,\ell,m\eta}, U^{(4h)}_{2,0;\jmath,\ell,m\eta}\right\} = \mathrm{i}(\sec^2\theta)\tfrac{\partial}{\partial\eta}\left\{H^{(2|4,-2)}_{0,2;\ell,m} W^{(2)}_{2,2;\jmath-\ell}, -H^{(2|-4,-2)^*}_{0,2;\ell,m} W^{(2)}_{2,2;\jmath+\ell}\right\}, \tag{7.47}$$

$$\mathcal{L}_2 U^{(4i)}_{2,0;\jmath,\ell\eta} = (\sec^2\theta)\left[G^{(3b|1,0:1,3,-1)}_{(\jmath-\ell)|1,1;\ell}\right]_\eta, \quad \mathcal{L}_2 U^{(4k)}_{2,0;\jmath,\ell,m,n\eta} = (\sec^2\theta)\left[G^{(3d|1,0:1,3,-1)}_{(\jmath-\ell)|1,1;\ell,m,n}\right]_\eta, \tag{7.48}$$

$$\mathcal{L}_2 U^{(4c/4j)}_{2,0;\jmath,\ell,m\eta} = (\sec^2\theta)\left[G^{(3a/3c|1,0:1,3,-1)}_{(\jmath-\ell)|1,1;\ell,m} - \tilde{G}^{(3a/3b|1,0:1,1,-1)}_{(-\jmath+\ell)|3,1;\ell,m}\right]_\eta, \tag{7.49}$$

$$\mathcal{L}_2 U^{(4l/4m)}_{2,0;\jmath,\ell,m,n\eta} = (\sec^2\theta)\left[G^{(3e/3f|1,0:1,3,-1)}_{(\jmath-\ell)|1,1;\ell,m,n} - \tilde{G}^{(3c/3d|1,0:1,1,-1)}_{(-\jmath+\ell)|3,1;\ell,m,n}\right]_\eta, \tag{7.50}$$

$$\mathcal{L}_2\left\{U^{(4n)}_{2,0;\jmath,\ell,m\eta}, U^{(4o)}_{2,0;\jmath,\ell,m,n\eta}\right\} = (\sec^2\theta)\tfrac{\partial}{\partial\eta}\left\{G^{(3g|1,0:1,3,-1)}_{(\jmath-\ell)|1,1;\ell,m}, G^{(3h|1,0:1,3,-1)}_{(\jmath-\ell)|1,1;\ell,m,n}\right\}, \tag{7.51}$$

and

$$V^{(k)}_{2,0;\jmath[,\ell,m,n]\eta\eta} = 2U^{(k)}_{2,0;\jmath[,\ell,m,n]\eta} + \mathcal{Y}^{(k)}_{2,0;\jmath[,\ell,m,n]} \quad \text{for} \quad k = 4L, 4a, \ldots, 4o, \tag{7.52}$$

where $\mathcal{R}^{(4a)}_{2,0;\jmath,\ell}$ in (7.45) and $\mathcal{Y}^{(4a)}_{2,0;\jmath,\ell}$ in (7.52) are given in Appendix C and $\mathcal{Y}^{(k)}_{2,0;\jmath[,\ell,m,n]} = 0$ if $k \neq 4a$. We have put

$$H^{(k|d_1,d_2)}_{a,b;\ell,m} \equiv \tfrac{\tau}{2}(\sin^2\theta)\left(d_1 U^{(k)}_{a,b;\ell,m} + d_2 W^{(k)}_{a,b;\ell,m} - V^{(k)}_{a,b;\ell,m}\tfrac{\partial}{\partial\eta}\right), \tag{7.53}$$

and we have also used (5.29), (7.3), (7.18) and (7.33). The equations for $U^{(4c)}_{2,0;\jmath,\ell,m\eta}$ and $U^{(4j)}_{2,0;\jmath,\ell,m\eta}$ are obtained from (7.49) by choosing the superscripts $\{3a, 3a\}$ and $\{3c, 3b\}$, respectively, and similarly the superscripts $\{3e, 3c\}$ are used for $U^{(4l)}_{2,0;\jmath,\ell,m,n\eta}$ and $\{3f, 3d\}$ are for $U^{(4m)}_{2,0;\jmath,\ell,m,n\eta}$ in (7.50).

The solutions of the above fourth-order equations must satisfy the following transverse boundary conditions:

$$U^{(k)}_{2,0;\jmath[,\ell,m,n]\eta} \to 0 \quad \text{as} \quad \eta \to \pm\infty, \tag{7.54}$$

for $k = 4L,\ 4a,\ \ldots,\ 4o$.

The above system of partial differential equations must be solved with the jump equations in order to obtain the streamwise evolution of $A_\jmath$ and $B_\jmath$. The jump equation for the oblique mode becomes from (6.30) and (6.32)

$$\begin{aligned}
&\left(\cos\theta + \frac{1}{\cos\theta}\right)\left[A_{\jmath\bar{x}} + \tfrac{\mathrm{i}}{2}(\jmath\bar{\chi} - \eta_o)A_\jmath\right] - \tfrac{1}{4}\xi(\sec^2\theta)\left(2\sigma^r\hat{\kappa}\tau_w\bar{\lambda}\right)^{1/2}A_\jmath \\
&= -\frac{\mathrm{i}}{4\pi\tau}(\sec^2\theta)\int_{-\infty}^{\infty} d\eta\left[V^{(3L)}_{1,1;\jmath\eta\eta} + V^{(3a)}_{1,1;0,\jmath\eta\eta} + V^{(3b)}_{1,1;\jmath\eta\eta} + V^{(3c)}_{1,1;\jmath,0\eta\eta} + V^{(3g)}_{1,1;\jmath,0\eta\eta}\right. \\
&\qquad\left. + \sum_{\ell=-J}^{J}\left(V^{(3d)}_{1,1;\jmath,\jmath-\ell,\ell\eta\eta} + V^{(3e)}_{1,1;\jmath,\jmath+\ell,\jmath\eta\eta} + V^{(3f)}_{1,1;\jmath,\jmath+\ell,\ell\eta\eta} + V^{(3h)}_{1,1;\jmath,\ell-\jmath,\jmath\eta\eta}\right)\right],
\end{aligned} \tag{7.55}$$

and the plane-wave jump equation becomes from (6.31) and (6.33)

$$\begin{aligned}
&B_{\jmath\bar{x}} + \mathrm{i}\,(\jmath\bar{\chi} - \eta_o)\,B_\jmath - \tfrac{1}{2}\xi\left(\sigma^r\hat{\kappa}\tau_w\bar{\lambda}\right)^{1/2}B_\jmath = -\frac{\mathrm{i}}{\pi\tau}\int_{-\infty}^{\infty} d\eta\left[\tfrac{1}{2}U^{(4L)}_{2,0;\jmath\eta} + U^{(4a)}_{2,0;2\jmath,\jmath\eta} + U^{(4b)}_{2,0;\jmath,0\eta}\right. \\
&\left. + U^{(4d)}_{2,0;\jmath,0\eta} + U^{(4i)}_{2,0;2\jmath,\jmath\eta} + \sum_{\ell=-J+\jmath}^{J+\jmath}\left(U^{(4c)}_{2,0;\jmath,\ell,\jmath\eta} + U^{(4e)}_{2,0;2\jmath,\ell,\jmath\eta} + U^{(4f)}_{2,0;2\jmath,\ell,(\ell-\jmath)\eta} + U^{(4g)}_{2,0;2\jmath,\ell,(\jmath-\ell)\eta}\right)\right.
\end{aligned}$$

$$+\sum_{\ell=-J-\jmath}^{J-\jmath} U^{(4h)}_{2,0;2\jmath,\ell,\jmath\eta}+\sum_{\ell=-J+2\jmath}^{J+2\jmath}\Big\{U^{(4j)}_{2,0;2\jmath,\ell,(\ell-\jmath)\eta}+U^{(4n)}_{2,0;2\jmath,\ell,(\jmath-\ell)\eta}$$
$$+\sum_{m=\max(-J+\jmath,-J+\ell)}^{\min(J+\jmath,J+\ell)}\Big(U^{(4k)}_{2,0;2\jmath,\ell,m,(\jmath-m)\eta}+U^{(4l)}_{2,0;2\jmath,\ell,m,\jmath\eta}+U^{(4m)}_{2,0;2\jmath,\ell,m,(m-\jmath)\eta}\Big)$$
$$+\sum_{m=\max(-J-\jmath,-J-\ell)}^{\min(J-\jmath,J-\ell)} U^{(4o)}_{2,0;2\jmath,\ell,m,\jmath\eta}\Big\}\Big], \quad (7.56)$$

where (5.23), (5.29), (7.1), (7.2), (7.4), (B 3) and (B 6) have been used along with

$$\xi \equiv \bar{\alpha}/(\tau_w \bar{c}), \quad (7.57)$$

and ξ (also in (C 11)) becomes unity, at the leading order, if we use (2.5), (5.8) and (5.9). The terms involving $\mathrm{i}\jmath\bar{\chi}$ on the left hand sides of (7.55) and (7.56) account for the wavenumber difference between the $\jmath$th and 0th resonant-triads (see (5.21)) which is caused by the frequency detuning introduced in (2.6). In this analysis, it is convenient to choose the transverse coordinate origin shift η_o introduced by (7.1) to be zero

$$\eta_o = 0. \quad (7.58)$$

The upstream flow can start out as a system of resonant-triads of linear instability waves (Goldstein & Lee 1992; Lee 1997a), as a system of resonant-triads of linear and nonlinear instability waves (Wundrow *et al.* 1994; Goldstein 1994; Lee 1997a) or as a system of pairs of nonlinear oblique modes (Wu *et al.* 1997). The upstream boundary condition in the linear instability-wave case becomes

$$A_\jmath \to \tilde{a}_\jmath \exp\left[(\kappa_{ob}-\tfrac{\mathrm{i}}{2}\jmath\bar{\chi})\bar{x}\right], \quad B_\jmath \to \tilde{b}_\jmath \exp\left[(\kappa_{2d}-\mathrm{i}\jmath\bar{\chi})\bar{x}\right] \qquad \text{as} \quad \bar{x}\to-\infty, \quad (7.59)$$

where

$$\tilde{a}_\jmath = \frac{\tilde{A}_0^{(0)}}{\hat{\kappa}\bar{c}}\left(\frac{Y_c}{\tilde{B}_0^{(0)}}\right)^{1/2}\left(\frac{\hat{\kappa}^4}{M|\tilde{B}_0^{(0)}|}\right)^{\kappa_{ob}/\kappa_{2d}-1/2}\exp\left(\tfrac{\mathrm{i}}{2}\jmath\hat{\kappa}\bar{\chi}x_o\right), \quad \tilde{b}_\jmath = \frac{\tilde{B}_\jmath^{(0)}}{\tilde{B}_0^{(0)}}\exp\left(\mathrm{i}\jmath\hat{\kappa}\bar{\chi}x_o\right), \quad (7.60)$$

$\bar{\chi}$ and M are given by (7.2) and (7.5) and we have used (5.23). The $\tilde{A}_j^{(0)}$ and $\tilde{B}_j^{(0)}$ are the complex initial values of the oblique and plane wave amplitudes $\tilde{A}_j$ and $\tilde{B}_j$ in (3.1) to (3.4),

$$\tilde{A}_j \to \tilde{A}_j^{(0)} \exp\left(\tfrac{1}{2}\hat{\kappa}\tau_w \bar{\alpha}\kappa_{ob} x_1\right), \quad \tilde{B}_j \to \tilde{B}_j^{(0)} \exp\left(\tfrac{1}{2}\hat{\kappa}\tau_w \bar{\alpha}\kappa_{2d} x_1\right) \quad \text{as} \quad x_1 \to -\infty. \tag{7.61}$$

The origin shifts x_0 and X_0 in (7.1) are chosen to satisfy

$$(M/\hat{\kappa}^4)\tilde{B}_0^{(0)} e^{\mathrm{i}X_0 + \hat{\kappa}\kappa_{2d}x_0} = 1. \tag{7.62}$$

The upstream matching conditions for a system of resonant-triads in the later stage of the critical-layer evolution can be obtained from the solutions of the preceding linear or nonlinear stages as in Wundrow *et al.* (1994), Goldstein (1994), Wu *et al.* (1997) and Lee (1997a).

The linear growth rates of the oblique and plane waves, κ_{ob} and κ_{2d}, can be obtained from (7.55) and (7.56),

$$\kappa_{ob} = \frac{\sec\theta}{4(1+\cos^2\theta)}\left[-\frac{\mathrm{i}}{\pi\tau A_j}\int_{-\infty}^{\infty} d\eta V_{1,1;j\eta\eta}^{(3L)} + \xi\left(2\sigma^r\hat{\kappa}\tau_w\bar{\lambda}\right)^{1/2}\right], \tag{7.63}$$

$$\kappa_{2d} = -\frac{\mathrm{i}}{2\pi\tau B_j}\int_{-\infty}^{\infty} d\eta U_{2,0;j\eta}^{(4L)} + \tfrac{1}{2}\xi\left(\sigma^r\hat{\kappa}\tau_w\bar{\lambda}\right)^{1/2}. \tag{7.64}$$

The last terms in both equations are due to the viscous Stokes-layer effect and this effect enhances the linear growth rates of the instability waves. Their magnitudes are of $O(\sigma^{r/2})$, but they will become $O(1)$ in the viscous limit where $\bar{\lambda} = O(\sigma^{-r})$.

It is easy to solve (7.22) and (7.44) to show that, as in Part 2,

$$\int_{-\infty}^{\infty} d\eta V_{1,1;j\eta\eta}^{(3L)} = 2\mathrm{i}\pi\bar{a}_{1M}^{(2)} A_j, \quad \int_{-\infty}^{\infty} d\eta U_{2,0;j\eta}^{(4L)} = 2\mathrm{i}\pi\bar{a}_{1M}^{(2)} B_j, \tag{7.65}$$

where $\bar{a}_{1M}^{(2)}$ is given by (7.3). As mentioned earlier, see (6.21), (6.23) and (7.3), $\bar{a}_{1M}^{(2)}$ (that is composed of two parts) is proportional to the double derivative of the base mean flow at

the critical level. The first term on the right hand side of (3.19) is due to the mean pressure gradient and the adverse pressure gradient (positive value of $\bar{\mu}$) increases the linear growth rate, while the second term, which is always negative, is due to the Blasius profile. In the later non-equilibrium critical-layer stage the exponent r of the growth-rate parameter σ^r is smaller than 3 and also $\bar{\mu} \ll 1$ as shown by Wundrow *et al.* (1994), Goldstein (1994), Wu *et al.* (1997) and Lee (1997a). Thus, from (3.19), the linear growth rates given by (7.63) and (7.64) become negligibly small compared to the nonlinear growth rates.

8. Concluding remarks

The non-equilibrium critical-layer analysis of a system of frequency-detuned resonant-triads is presented. It is shown that resonant-triads can interact nonlinearly between themselves in the common critical layer if the scaled Strouhal numbers (of their fundamental plane waves) are different by the magnitude of the growth-rate parameter, $O(\sigma^r)$. The flow outside the critical layer is still governed by the linear dynamics. The generalized scaling of Lee (1997a) has been used for the long-wavelength small-growth-rate instability modes in boundary layers with and without mean pressure gradient. The wavenumber parameter σ characterizes the small wavenumber and the growth-rate parameter σ^r characterizes the ratio of the small growth rate to the wavenumber of the instability wave. Although the analysis was carried out with the non-equilibrium critical-layer scaling, the quasi-equilibrium amplitude equations can be obtained in Part 2 by taking the viscous limit of the finite-viscosity amplitude equations. It was shown by Goldstein (1994), Wu *et al.* (1997) and Lee (1997a) that the later downstream stage of the quasi-equilibrium critical-layer evolution is governed by the non-equilibrium dynamics. In fact, the final critical-layer stage will be

governed by the inviscid version of the system of equations presented in §7 without the linear growth terms. Since the value of r becomes nearly equal to zero there, the viscous effect and the linear growth rate will become negligibly small (Wundrow *et al.* 1994).

The effect of the viscous Stokes layer has been included so that the linear growth rates are valid for both in the finite-viscosity and viscous-limit cases. The upstream instability waves can be composed of either linear instability waves or nonlinear waves of the preceding critical-layer stage.

The nonlinear effect in the critical layer produces a term which is periodic in the spanwise direction with the spanwise wavenumber equal to twice of that of the oblique modes. In contrast to the previous results (Goldstein & Choi 1989; Goldstein & Lee 1992, 1993; Wu 1992, 1993; Leib & Lee 1995), this term becomes unsteady in the present multi-frequency-interaction case. The magnitude of this nonlinearly generated low-frequency mode is as large as that of the primary oblique modes outside the critical layer. The complete solutions of the spanwise-periodic components, as details will be given in Part 2, can be obtained from the multi-layer analysis as in Wu (1993). When $r = 3$ and λ defined by (2.8) is $O(1)$, we need to consider the solutions in the potential region where $y = \tilde{y}/\sigma$, the main boundary layer where $y = O(1)$ and the viscous wall layer where $y = \sigma^3\hat{Y}$ in addition to the inviscid wall layer of $O(\sigma)$ and the critical layer of $O(\sigma^4)$. The viscous wall layer, which is thicker than the viscous Stokes layer in §4, is required in order to satisfy the wall boundary conditions. (The inviscid-wall-layer solutions of the streamwise and spanwise components become singular at the wall.) The three-dimensional boundary-layer equations in the viscous wall layer must be solved with the no-slip boundary conditions at the wall and appropriate boundary conditions on the upper edge of the layer in order to match with the

solutions in the inviscid wall layer. The transverse velocity on the upper edge of the viscous wall layer is determined internally by the boundary-layer equations themselves and it can not be given as a boundary condition as in Wu (1993). It is interesting to find out that the velocity components in the inviscid wall layer, at the leading order, become equal to zero where $Y > Y_c$ but non-zero where $Y < Y_c$ (Lee 1997c). Thus, the nonlinear interaction between oblique modes produces, at the leading order, the spanwise-periodic velocities only below the critical layer. The non-zero velocities at $Y = Y_{c-}$ will be determined from the matching with the critical-layer jumps.

Since the velocity jumps of these low-frequency modes across the critical layer are determined from the solutions of the amplitude equations, which become singular at a finite downstream position, the magnitude of the spanwise-periodic velocities also becomes very large near the singular point. When r becomes $9/10$ the streamwise velocity becomes as big as the base mean flow, therefore, the nonlinearly generated spanwise-periodic component and the base mean flow start to interact nonlinearly in the viscous wall layer whose thickness is of $O(\sigma^{37/10})$ (Part 2; Lee 1997c). This nonlinear viscous wall layer will be separated into two layers (inviscid nonlinear layer and the viscous nonlinear layer) in the later downstream region.

When the difference between the scaled Strouhal numbers, $\bar{s}_j$ given by (2.5), of the resonant-triads is larger than the magnitude of the growth-rate parameter σ^r, the instability waves of an individual resonant-triad initially grow independently of the instability modes of the other resonant-triads. For example, when $r = 3$ in the adverse-pressure-gradient boundary layer (Goldstein & Lee 1992), the plane and oblique waves of the resonant-triad I (and those of the resonant-triad II) go through the usual linear stage, parametric-resonance

stage and the fully coupled stage, independently of the other resonant-triad, as shown in figure 2, provided the (fundamental) frequency of the resonant-triad II is larger than that of the resonant-triad I by $O(\sigma^{\rho+2})$, where ρ is a positive number that is smaller than 3. Since the distance between the critical levels, $y_{cII} - y_{cI}$, which is of $O(\sigma^{\rho+1})$, is larger than the critical-layer thickness of $O(\sigma^4)$, the growth of each resonant-triad is not affected by the presence of the other resonant-triad. The streamwise evolution of the oblique and plane waves are still determined by the integro-differential amplitude equations (5.50) and (5.51) of Goldstein & Lee (1992), or by the $O(1)$-viscosity equations given by Wu (1995) and Lee (1997a).

The non-equilibrium critical layer becomes thicker and r becomes smaller as the instability waves propagate downstream (Goldstein & Lee 1992; Wundrow *et al.* 1994; Goldstein 1994; Wu *et al.* 1997; Lee 1997a) mainly due to the self-interaction between oblique modes. The instability modes of different resonant-triads start to interact nonlinearly within their overlapped critical layers when r becomes equal to ρ. The oblique and plane waves of both resonant-triads I and II in figure 2 become fully coupled in the frequency-detuned nonlinear-interaction stage where their growth rates are now $O(\sigma^{\rho+1})$, or $r = \rho(< 3)$, which is the initial difference between the respective critical levels. The amplitudes are then determined by the inviscid version of the system of equations presented in §7. When r approaches to zero the critical layer becomes almost as thick as the inviscid wall layer whose thickness is of $O(\sigma)$ and, thus, a wide range of instability waves with the scaled frequencies differing by almost $O(1)$ can now nonlinearly interact between themselves. This non-equilibrium critical-layer stage is still governed by the parabolic type equations of this paper, but the flow in the next stage will be governed by fully elliptic triple-deck equations (Goldstein &

Lee 1992, 1993; Wu *et al.* 1997). The turbulent flow field may be determined by solving these elliptic equations with the upstream matching boundary conditions that can be obtained from the solutions of the equations presented in §7 (with appropriate downstream boundary conditions).

The system of critical-layer equations are presented in §7. The variables are normalized (Lee 1997a) in such a way that the mean-flow-dependent parameters, i.e. $\bar{a}_{1M}^{(2)}$ and τ_w, only appear in the linear growth rate terms in (7.63) and (7.64) or in (7.22), (7.44), (7.55) and (7.56). We can show that $\bar{a}_M^{(1)}$, $\bar{a}_{2M}^{(2)}$, $\bar{a}_{3M}^{(2)}$ and $\bar{b}_M^{(2)}$ in (C 1), (C 2), (C 4), (C 5) and (C 7) do not play any major role in computing the velocity jump across the critical layer and they will not appear in the final amplitude equations (Goldstein & Lee 1992; Lee 1997a). The nonlinear part of the system of critical-layer equations is free from any mean-flow-dependent parameters except $\bar{\lambda}$. Therefore, the results of this frequency-detuned analysis can be universally applied to other shear flows, with minor modifications for the specific linear growth rates, which have been individually studied for the single resonant-triad or single-frequency oblique modes, for example, oscillatory Stokes flows by Wu (1992, 1995) and Wu *et al.* (1993), free shear layers by Goldstein & Choi (1989) and Mallier & Maslowe (1994) and supersonic boundary layers by Leib & Lee (1995). The magnitude of the wavenumber of the instability wave in these analyses is of order one and thus the near-neutral small-growth-rate approximation that was originally introduced by Goldstein & Leib (1988) and Goldstein & Hultgren (1988) has to be used instead of the long-wavelength small-growth-rate approximation used in this analysis. The nonlinear part of the system of critical-layer equations is also valid for any values of θ (for the oblique-mode interactions) since the resonance relation (5.15) or (5.16) has not been used in it.

The frequencies of the fundamental plane waves of the frequency-detuned resonant-triads can be freely specified (or can be given by experiments). The small parameter σ, which accounts for the small wavenumber of the instability waves in boundary-layer flows, can be chosen from the adverse-pressure-gradient boundary-layer scaling (Goldstein *et al.* 1987; Goldstein & Lee 1992; Wundrow *et al.* 1994), the upper-branch scaling (Mankbadi *et al.* 1993; Goldstein 1994; Wu *et al.* 1997), or the favorable-pressure-gradient boundary-layer scaling (Wu 1993). The scaled Strouhal number $\bar{s}_j$ and the frequency-detuning factor χ are then computed from (2.5) and (2.6). The wavenumber of the plane wave $\bar{\alpha}_j$ that possess the series expansion (5.8) is fully determined by the dispersion relations (5.9) to (5.13) and the phase speed $\bar{c}_j$ can be obtained from (2.5). The wavenumbers $\bar{\beta}_j$ and $\bar{\gamma}_j$ of the oblique modes are computed from (5.15), (5.16) and (5.18). In order to obtain the streamwise evolution of the (complex) oblique and plane wave amplitudes A_j and B_j of the full system of resonant-triads, the system of partial differential critical-layer equations in §7 must be solved with the jump equations (7.55) and (7.56) along with the upstream conditions (7.59). However, we only need to solve (7.8) – (7.16), (7.20), (7.22) – (7.32) and (7.34) with (7.55) and (7.59) for the nonlinear interaction between the frequency-detuned pairs of oblique modes.

The system of partial differential critical-layer equations can be solved both analytically (Goldstein & Choi 1989; Goldstein & Lee 1992, 1993; Wu 1992, 1995; Wu *et al.* 1993) and numerically (Lee 1997a). It may be more convenient to solve them numerically for the finite-viscosity resonant-triad case. But it is relatively simple to solve them analytically when only the pairs of oblique modes are considered. The resulting analytical amplitude equations, as will be given in Part 2, are quite compact and can be easily solved numerically.

Comparison with the analyses of Goldstein & Lee (1992) and Lee (1997a) shows that the previously considered single-resonant-triad is a special case of the present multi-resonant-triads. The perfectly tuned case of Goldstein & Lee (1992) and Lee (1997a), when $\bar{\kappa}_i$ in (8.3) of Lee (1997a) is equal to zero, corresponds to the interaction of a single 0th resonant-triad, i.e. between the 0th plane wave and the pair of 0th oblique modes.

The system of partial differential critical-layer equations in §7 will be solved analytically and the amplitude equations (without the back-reaction term in the plane-wave amplitude equation) and their viscous limit will be presented in Part 2 (Lee 1998b) along with the numerical solutions. The low-frequency spanwise-periodic components that are induced by the nonlinear effects in the critical layer will also be considered in Part 2.

This work was supported by the Acoustics Branch at NASA Lewis Research Center, contract number NAS3-98022.

Appendix A. Governing equations for $u^{(l)}$, $\bar{v}^{(l)}$, $w^{(l)}$ and $p^{(l)}$

$$\bar{\alpha}u_X^{(1)} + \bar{\beta}w_Z^{(1)} = 0, \tag{A 1}$$

$$\bar{\alpha}u_X^{(k)} + u_{x_1}^{(k-1)} + \bar{v}_{\bar{\eta}}^{(k)} + \bar{\beta}w_Z^{(k)} + \tfrac{\sqrt{3}}{4}\tilde{\chi}\bar{\alpha}w_{z_1}^{(k-1)} = 0 \quad \text{for} \quad k = 2, 3 \text{ and } 4, \tag{A 2}$$

$$Lu^{(1)} = \sum_{j=-J}^{J} \mathrm{Re}\, 2\mathrm{i}\tau_w\bar{\gamma}\bar{c}(\sin^2\theta)\bar{A}_j\tilde{E}_{cj}, \tag{A 3}$$

$$Lw^{(1)} = \sum_{j=-J}^{J} \mathrm{Re}\,\tau_w\bar{\alpha}\bar{c}(\sin\theta)\bar{A}_j\tilde{E}_{sj}, \tag{A 4}$$

$$Lu_{\bar{\eta}}^{(2)} = u_{\bar{\eta}\bar{\eta}}^{(1)} \sum_{j=-J}^{J} \mathrm{Re}\, 2\mathrm{i}\tau_w Y_c\bar{\gamma}\bar{A}_j\tilde{E}_{cj} + \tau_w\left(\bar{\beta}w_Z^{(2)} - \bar{\eta}u_{\bar{\eta}x_1}^{(1)} + \tfrac{\sqrt{3}}{4}\tilde{\chi}\bar{\alpha}w_{z_1}^{(1)}\right) - \left(\bar{\alpha}u^{(1)}u_X^{(1)} + \bar{\beta}w^{(1)}u_Z^{(1)}\right)_{\bar{\eta}}, \tag{A 5}$$

$$Lw^{(2)} = \sum_{j=-J}^{J} \tau_w \bar{\gamma} \left[\sqrt{3} j \tilde{\chi} \bar{c} (\cos^2\theta) \mathrm{Re}\, \bar{A}_j \tilde{E}_{sj} + w_{\bar{\eta}}^{(1)} \mathrm{Re}(2\mathrm{i} Y_c \bar{A}_j \tilde{E}_{cj}) \right] - \bar{\beta} p_Z^{(2)} - \tau_w \bar{\eta} w_{x_1}^{(1)}$$
$$- \bar{\alpha} u^{(1)} w_X^{(1)} - \bar{\beta} w^{(1)} w_Z^{(1)}, \qquad \text{(A 6)}$$

$$Lu_{\bar{\eta}}^{(3)} = u_{\bar{\eta}\bar{\eta}}^{(2)} \sum_{j=-J}^{J} \mathrm{Re} 2\mathrm{i} \tau_w Y_c \bar{\gamma} \bar{A}_j \tilde{E}_{cj} + \tau_w \left(\bar{\beta} w_Z^{(3)} - \bar{\eta} u_{\bar{\eta} x_1}^{(2)} \right) + \tfrac{\sqrt{3}}{4} \tilde{\chi} \bar{\alpha} \left[\tau_w w_{z_1}^{(2)} - \left(w^{(1)} u_{z_1}^{(1)} \right)_{\bar{\eta}} \right]$$
$$- \left[u^{(1)} u_{x_1}^{(1)} + u_{\bar{\eta}}^{(1)} \bar{v}^{(2)} + \bar{\alpha} \left(u^{(1)} u^{(2)} \right)_X + \bar{\beta} \left(w^{(1)} u_Z^{(2)} + w^{(2)} u_Z^{(1)} \right) \right]_{\bar{\eta}}, \qquad \text{(A 7)}$$

$$Lw^{(3)} = w_{\bar{\eta}}^{(2)} \sum_{j=-J}^{J} \mathrm{Re} 2\mathrm{i} \tau_w Y_c \bar{\gamma} \bar{A}_j \tilde{E}_{cj} - \bar{\beta} p_Z^{(3)} - \tfrac{\sqrt{3}}{4} \tilde{\chi} \bar{\alpha} \left(p_{z_1}^{(2)} + w^{(1)} w_{z_1}^{(1)} \right) - \tau_w \eta w_{x_1}^{(2)}$$
$$- u^{(1)} w_{x_1}^{(1)} - \bar{v}^{(2)} w_{\bar{\eta}}^{(1)} - \bar{\alpha} \left(u^{(1)} w_X^{(2)} + u^{(2)} w_X^{(1)} \right) - \bar{\beta} \left(w^{(1)} w^{(2)} \right)_Z, \qquad \text{(A 8)}$$

$$Lu_{\bar{\eta}}^{(4)} = u_{\bar{\eta}\bar{\eta}}^{(3)} \sum_{j=-J}^{J} \mathrm{Re} 2\mathrm{i} \tau_w Y_c \bar{\gamma} \bar{A}_j \tilde{E}_{cj} + \tau_w \left(\bar{\beta} w_Z^{(4)} - \bar{\eta} u_{\bar{\eta} x_1}^{(3)} \right)$$
$$+ \tfrac{\sqrt{3}}{4} \tilde{\chi} \bar{\alpha} \left[\tau_w w_{z_1}^{(3)} - \left(w^{(1)} u_{z_1}^{(2)} + w^{(2)} u_{z_1}^{(1)} \right)_{\bar{\eta}} \right] - \left[\left(u^{(1)} u^{(2)} \right)_{x_1} + u_{\bar{\eta}}^{(1)} \bar{v}^{(3)} + u_{\bar{\eta}}^{(2)} \bar{v}^{(2)} \right.$$
$$\left. + \bar{\alpha} \left(u^{(1)} u^{(3)} + \tfrac{1}{2} u^{(2)} u^{(2)} \right)_X + \bar{\beta} \left(w^{(1)} u_Z^{(3)} + w^{(2)} u_Z^{(2)} + w^{(3)} u_Z^{(1)} \right) \right]_{\bar{\eta}}, \qquad \text{(A 9)}$$

and

$$p_{\bar{\eta}}^{(k)} = 0 \quad \text{for} \quad k = 2 \text{ and } 3, \qquad \text{(A 10)}$$

where we have put

$$L \equiv \bar{c} \left(\frac{\partial}{\partial x_1} + \chi \bar{\alpha} \frac{\partial}{\partial t_1} \right) + \tau_w \bar{\alpha} \bar{\eta} \frac{\partial}{\partial X} - \lambda \frac{\partial^2}{\partial \bar{\eta}^2}, \qquad \text{(A 11)}$$

$\tilde{E}_{cj}$ and $\tilde{E}_{sj}$ are defined by (5.34), $\tilde{\chi}$ and χ are related by (5.23) and θ is defined in (5.29). We have also used (3.8) and (3.20).

Appendix B. Variables in the normalized critical-layer equations in §7

$$q_{1,1;j}^{(2L)} = \frac{(Y_c M)^{1/2} \cos\theta}{\hat{\kappa}^3 \tau_w \bar{c}} \mathcal{D}_{1;j} \tilde{q}_{1,1;j}^{(2L)}, \quad q_{2,0;j}^{(2L)} = \frac{\bar{c} M}{2\hat{\kappa}^3 \tau_w Y_c} \mathcal{D}_{2;2j} \tilde{q}_{2,0;j}^{(2L)}, \qquad \text{(B 1)}$$

$$\left\{q^{(2)}_{0,0;\jmath},\, q^{(2)}_{0,2;\jmath,\ell},\, q^{(2)}_{2,0;\jmath,\ell},\, q^{(2)}_{2,2;\jmath}\right\} = \frac{M}{\hat{\kappa}^3\tan^2\theta}\left\{\mathcal{D}_{0;\jmath}\tilde{q}^{(2)}_{0,0;\jmath},\, \mathcal{D}_{0;\jmath}\tilde{q}^{(2)}_{0,2;\jmath,\ell},\, \mathcal{D}_{2;\jmath}\tilde{q}^{(2)}_{2,0;\jmath,\ell},\, \mathcal{D}_{2;\jmath}\tilde{q}^{(2)}_{2,2;\jmath}\right\}, \quad \text{(B 2)}$$

$$\left\{q^{(3a)}_{1,1;\jmath,\ell},\, q^{(k)}_{1,1;\jmath[,\ell,m]}\right\} = \frac{\bar{c}M^{3/2}\cos\theta}{\hat{\kappa}^4 Y_c^{1/2}\tan^2\theta}\left\{\mathcal{D}_{1;\jmath+\ell}\tilde{q}^{(3a)}_{1,1;\jmath,\ell},\, \mathcal{D}_{1;\jmath}\tilde{q}^{(k)}_{1,1;\jmath[,\ell,m]}\right\} \quad \text{for} \quad k = 3L, 3b, \ldots, 3h, \quad \text{(B 3)}$$

$$q^{(3L)}_{2,0;\jmath} = \frac{M}{\hat{\kappa}^4\tau_w}\mathcal{D}_{2;2\jmath}\tilde{q}^{(3L)}_{2,0;\jmath}, \qquad q^{(3)}_{2,0;\jmath,\ell} = \frac{M\cos^2\theta}{\hat{\kappa}^4\tau_w}\mathcal{D}_{2;\jmath}\tilde{q}^{(3)}_{2,0;\jmath,\ell}, \quad \text{(B 4)}$$

$$\left\{q^{(3a)}_{3,1;\jmath,\ell},\, q^{(3b,3c,3d)}_{3,1;\jmath,\ell[,m]}\right\} = \frac{\bar{c}M^{3/2}\cos\theta}{\hat{\kappa}^4 Y_c^{1/2}\tan^2\theta}\left\{\mathcal{D}_{3;\jmath+\ell}\tilde{q}^{(3a)}_{3,1;\jmath,\ell},\, \mathcal{D}_{3;\jmath}\tilde{q}^{(3b,3c,3d)}_{3,1;\jmath,\ell[,m]}\right\}, \quad \text{(B 5)}$$

$$\left\{q^{(4L)}_{2,0;\jmath},\, q^{(4b)}_{2,0;\jmath,\ell},\, q^{(4c)}_{2,0;\jmath,\ell,m},\, q^{(4d)}_{2,0;\jmath,\ell},\, q^{(k)}_{2,0;\jmath,\ell[,m,n]}\right\} = \frac{2\pi\bar{\alpha}M}{\hat{\kappa}^5\tau_w^3\bar{c}}\left\{\mathcal{D}_{2;2\jmath}\tilde{q}^{(4L)}_{2,0;\jmath},\, \mathcal{D}_{2;2\jmath-\ell}\tilde{q}^{(4b)}_{2,0;\jmath,\ell},\right.$$
$$\left.\mathcal{D}_{2;\jmath+m}\tilde{q}^{(4c)}_{2,0;\jmath,\ell,m},\, \mathcal{D}_{2;2\jmath+\ell}\tilde{q}^{(4d)}_{2,0;\jmath,\ell},\, \mathcal{D}_{2;\jmath}\tilde{q}^{(k)}_{2,0;\jmath,\ell[,m,n]}\right\} \quad \text{for} \quad k = 4a, 4e, \ldots, 4o, \quad \text{(B 6)}$$

where M and $\mathcal{D}_{a;\jmath}(\bar{x})$ are given in (7.5) and (7.6) and θ is defined by (5.29). The normalization pair $\{q,\tilde{q}\}$ of $\{q^{(k)}_{a,b;\jmath[,\ell,m,n]}, \tilde{q}^{(k)}_{a,b;\jmath[,\ell,m,n]}\}$ for $k = 2L,\ 2,\ \ldots,\ 4o$ denotes either $\{U,\tilde{U}\}$, $\{V, 2\mathrm{i}\tilde{V}/(\hat{\kappa}\bar{\alpha}\bar{c})\}$, $\{W,\tilde{W}\tan\theta\}$ or $\{P,\mathrm{i}\tilde{P}(\tan^2\theta)/(\hat{\kappa}\tau_w\bar{c})\}$.

Appendix C. $W^{(2M)}_{1,1;\jmath}$ in (7.12); $W^{(3M)}_{1,1;\jmath}$ in (7.22); $\mathcal{R}^{(3L)}_{1,1;\jmath}$ in (7.31); $\mathcal{Z}^{(3)}_{2,0;\jmath,\ell}$, $\mathcal{R}^{(3)}_{2,0;\jmath,\ell}$ and $\mathcal{Y}^{(3)}_{2,0;\jmath,\ell}$ in (7.36); $\mathcal{R}^{(4a)}_{2,0;\jmath,\ell}$ in (7.45); $\mathcal{Y}^{(4a)}_{2,0;\jmath,\ell}$ in (7.52)

$$W^{(2M)}_{1,1;\jmath} = g_s\left(\mathcal{D}^{(\jmath:1,\sin^2\theta)}_{\bar{x}}\mathcal{D}^{(2)}_{\eta} + \jmath g_t\right)Q^{(1)}_{\jmath}, \quad \text{(C 1)}$$

$$W^{(3M)}_{1,1;\jmath} = 2\mathrm{i}\pi\xi\left(\mathcal{D}^{(\jmath:1,1)}_{\bar{x}}\mathcal{D}^{(2)}_{\eta} + \jmath g_t\right)\left[W^{(2L)}_{1,1;\jmath} + \jmath g_t g_s Q^{(1)}_{\jmath}\right] + \mathrm{i}\pi\xi g_s\left[\left(\mathcal{D}^{(\jmath:1,1)}_{\bar{x}}\right)^2\left\{\left(\hat{\eta}\mathcal{D}^{(2)}_{\eta}Q^{(1)}_{\jmath}\right)_{\eta}\right.\right.$$
$$\left.+\tfrac{2}{3}\mathrm{i}\bar{\lambda}\left(4+\mathcal{D}^{(2)}_{\eta}\right)Q^{(1)}_{\jmath\eta\eta\eta}\right\} - 2\mathrm{i}\bar{a}^{(1)}_{M}\mathcal{D}^{(\jmath:1,0)}_{\bar{x}}\mathcal{D}^{(2)}_{\eta}Q^{(1)}_{\jmath}\Big] + \mathrm{i}\tau g_s\left[\bar{a}^{(2)}_{2M}\mathcal{D}^{(2)}_{\eta} + \bar{a}^{(2)}_{3M}\left(\hat{x}\tfrac{\partial}{\partial\eta} - \tfrac{\mathrm{i}}{2}\tfrac{\partial^2}{\partial\eta^2}\right)\right.$$
$$\left.-\tfrac{\mathrm{i}}{2}\bar{b}^{(2)}_{M}\tfrac{\partial^2}{\partial\eta^2} + \bar{a}^{(2)}_{1M}\left\{\hat{\eta}\mathcal{D}^{(2)}_{\eta} + \mathrm{i}\bar{\lambda}\left(1+\tfrac{2}{3}\mathcal{D}^{(12/5)}_{\eta}\right)\tfrac{\partial^2}{\partial\eta^2}\right\}\right]Q^{(1)}_{\jmath}, \quad \text{(C 2)}$$

$$\mathcal{R}^{(3L)}_{1,1;\jmath} = 2\pi\mathrm{i}\xi\left(\mathcal{D}^{(\jmath:1,0)}_{\bar{x}}U^{(2L)}_{1,1;\jmath} + \jmath g_t W^{(2L)}_{1,1;\jmath}\right), \quad \text{(C 3)}$$

$$\mathcal{Z}^{(3)}_{2,0;\jmath,\ell} = \mathrm{i}(\jmath-2\ell)g_t g_s P^{(2)}_{2,0;\jmath,\ell} - G^{(2L|0,1:1,0,0)}_{(\jmath-\ell)|1,1;\ell}$$
$$-g_s\left[\hat{\eta}\mathcal{D}^{(\jmath:2,2)}_{\bar{x}}W^{(2)}_{2,0;\jmath,\ell} + \tfrac{\tau}{2}Q^{(1)}_{\jmath-\ell}\left(V^{(2L)}_{1,1;\ell\eta} - 2g_s\mathcal{D}^{(\ell:1,0)}_{\bar{x}}Q^{(1)}_{\ell}\right)\right], \tag{C 4}$$

$$\mathcal{R}^{(3)}_{2,0;\jmath,\ell} = (\jmath-2\ell)g_t g_s W^{(2)}_{2,0;\jmath,\ell} + \left[G^{(2L|1,0:1,0,-4)}_{(\jmath-\ell)|1,1;\ell}\right]_\eta - g_s\hat{\eta}\mathcal{D}^{(\jmath:2,2)}_{\bar{x}}Q^{(2)}_{2,0;\jmath,\ell}$$
$$+\tfrac{\tau}{2}g_s\left[\left\{3V^{(2L)}_{1,1;\ell\eta} - 2g_s\left(\mathcal{D}^{(\ell:1,0)}_{\bar{x}} - 2\ell g_t\right)Q^{(1)}_{\ell}\right\}Q^{(1)}_{\jmath-\ell}\right]_\eta, \tag{C 5}$$

$$\mathcal{Y}^{(3)}_{2,0;\jmath,\ell} = -\mathrm{i}g_s\left[\mathcal{D}^{(\jmath:2,0)}_{\bar{x}}U^{(2)}_{2,0;\jmath,\ell} + (\jmath-2\ell)g_t W^{(2)}_{2,0;\jmath,\ell}\right], \tag{C 6}$$

$$\mathcal{R}^{(4a)}_{2,0;\jmath,\ell} = -2\pi\xi g_e\left[\hat{\eta}\left(\bar{a}^{(1)}_M g_s\mathcal{D}^{(\jmath:2,0)}_{\bar{x}}Q^{(2)}_{2,0;\jmath,\ell} + \mathcal{D}^{(\jmath:2,2)}_{\bar{x}}Q^{(3)}_{2,0;\jmath,\ell}\right) - (\jmath-2\ell)g_t\left(\bar{a}^{(1)}_M g_s W^{(2)}_{2,0;\jmath,\ell}\right.\right.$$
$$\left.\left.+W^{(3)}_{2,0;\jmath,\ell}\right)\right] - \tau g_n\left[\left(\bar{a}^{(2)}_{1M}\hat{\eta}^2 + \bar{a}^{(2)}_{2M}\hat{\eta} + \bar{a}^{(2)}_{3M}\hat{x} - \tfrac{\mathrm{i}}{2}\bar{b}^{(2)}_M\tfrac{\partial}{\partial\eta}\right)U^{(2)}_{2,0;\jmath,\ell\eta} - \bar{a}^{(2)}_{1M}V^{(2)}_{2,0;\jmath,\ell}\right]$$
$$+g_e\left[G^{(3L|1,0:1,3,-1)}_{(\jmath-\ell)|1,1;\ell}\right]_\eta - \pi\xi g_n\left[\tfrac{\tau}{2}\left\{\left(\mathcal{D}^{(\jmath:2,0)}_{\bar{x}} + g_t\ell\right)U^{(2L)}_{1,1;\ell} + U^{(2L)}_{1,1;\ell}\tfrac{\partial}{\partial\bar{x}}\right.\right.$$
$$\left.\left.-(\jmath-\ell)g_t W^{(2L)}_{1,1;\ell}\right\}Q^{(1)}_{\jmath-\ell} + g_s^{-2}H^{(2L|1,-1)}_{1,1;\ell}U^{(2L)}_{1,1;\jmath-\ell}\right]_\eta, \tag{C 7}$$

$$\mathcal{Y}^{(4a)}_{2,0;\jmath,\ell} = -2\pi\mathrm{i}\xi g_e\left[\mathcal{D}^{(\jmath:2,0)}_{\bar{x}}U^{(3)}_{2,0;\jmath,\ell} + (\jmath-2\ell)g_t W^{(3)}_{2,0;\jmath,\ell}\right]_\eta, \tag{C 8}$$

where $\bar{\lambda}$, $\bar{a}^{(2)}_{1M}$, τ, $G^{(k|d_1,d_2:d_3,d_4,d_5)}_{(\jmath)|a,b;\ell[,m,n]}$ and $H^{(2L|1,-1)}_{1,1;\ell}$ are given in (7.2), (7.3), (7.18), (7.33) and (7.53). We have also put

$$\mathcal{D}^{(\jmath:a,b)}_{\bar{x}} \equiv \tfrac{\partial}{\partial\bar{x}} + \mathrm{i}\left(\jmath\bar{\chi} - \tfrac{1}{2}a\eta_o\right) + \mathrm{i}b\bar{a}^{(1)}_M, \quad \mathcal{D}^{(a)}_{\eta} \equiv \hat{\eta}\tfrac{\partial}{\partial\eta} + \tfrac{1}{3}\mathrm{i}a\bar{\lambda}\tfrac{\partial^3}{\partial\eta^3}, \tag{C 9}$$

$$\hat{\eta} \equiv \eta + \tfrac{1}{2}\eta_o, \quad \hat{x} \equiv \bar{x} + \kappa x_o, \tag{C 10}$$

$$\xi \equiv \bar{\alpha}/(\tau_w\bar{c}), \quad g_t \equiv \tfrac{\sqrt{3}}{2}\mathrm{i}\hat{\chi}\cot\theta, \quad g_s \equiv \sin^2\theta, \quad g_e \equiv \sec^2\theta, \quad g_n \equiv 2\mathrm{i}\tan^2\theta, \tag{C 11}$$

where ξ becomes unity, at the leading order, if we use (2.5), (5.8) and (5.9). The mean flow coefficients are normalized by

$$\bar{a}^{(1)}_M = \frac{a^{(1)}_M}{\hat{\kappa}\tau_w^2}, \quad \left\{\bar{a}^{(2)}_{2M}, \bar{a}^{(2)}_{3M}, \bar{b}^{(2)}_M\right\} = \frac{2\pi Y_c\bar{\alpha}}{\hat{\kappa}^2\tau_w^3\bar{c}^2}\left\{a^{(2)}_{2M}, \frac{2a^{(2)}_{3M}}{\hat{\kappa}^2\tau_w\bar{\alpha}\bar{c}}, \frac{2b^{(2)}_M}{\hat{\kappa}^2\bar{\alpha}\bar{c}^2}\right\}, \tag{C 12}$$

where $a^{(1)}_M$, $a^{(2)}_{2M}$, $a^{(2)}_{3M}$ and $b^{(2)}_M$ are defined in (6.12), (6.21) and (6.24) and $a^{(1)}_M$ is given in (6.13).

References

[1] BENNEY, D.J. & BERGERON, R.F. 1969 A new class of nonlinear waves in parallel flows. *Stud. Appl. Maths* **48**, 181-204.

[2] COWLEY, S.J. & WU, X. 1994 Asymptotic approaches to transition modelling. in *Progress in Transition Modelling*, AGARD Report 793, Chapter 3, 1-38.

[3] DRAZIN, P.G. & REID, W.H. 1981 *Hydrodynamic Stability.* Cambridge University Press.

[4] GOLDSTEIN, M.E. 1994 Nonlinear interactions between oblique instability waves on nearly parallel shear flows. *Phys. Fluids* **6**, 724-735.

[5] GOLDSTEIN, M.E. 1995 The role of nonlinear critical layers in boundary layer transition. *Phil. Trans. R. Soc. Lond. A* **352**, 425-442.

[6] GOLDSTEIN, M.E. 1996 The role of nonlinear critical layers in transition to turbulence in boundary layers. *AIAA Paper* 2122.

[7] GOLDSTEIN, M.E. & CHOI, S.W. 1989 Nonlinear evolution of interacting oblique waves on two–dimensional shear layers. *J. Fluid Mech.* **207**, 97-120. Also Corrigendum, *J. Fluid Mech.* **216**, 659-663.

[8] GOLDSTEIN, M.E., DURBIN, P.A. & LEIB, S.J. 1987 Roll–up of vorticity in adverse–pressure–gradient boundary layers. *J. Fluid Mech.* **183**, 325-342.

[9] GOLDSTEIN, M.E. & HULTGREN, L.S. 1988 Nonlinear spatial evolution of an externally excited instability wave in a free shear layer. *J. Fluid Mech.* **197**, 295-330.

[10] GOLDSTEIN, M.E. & LEE, S.S. 1992 Fully coupled resonant-triad interaction in an adverse-pressure-gradient boundary layer. *J. Fluid Mech.* **245**, 523-551.

[11] GOLDSTEIN, M.E. & LEE, S.S. 1993 Oblique instability waves in nearly parallel shear flows, in *Nonlinear Waves and Weak Turbulence with Applications in Oceanography and Condensed Matter Physics*, (eds. Fitzmaurice, N., Gurarie, D., McCaughan, F. & Woyczynski, W.), Birkhauser, 159-177.

[12] GOLDSTEIN, M.E. & LEIB, S.J. 1988 Nonlinear roll-up of externally excited free shear layers. *J. Fluid Mech.* **191**, 481-515.

[13] GRAEBEL, W.P. 1966 On determination of the characteristic equations for the stability of parallel flows. *J. Fluid Mech.* **24**, 497-508.

[14] HABERMAN, R. 1972 Critical layers in parallel flows. *Stud. Appl. Math.* **51**, 139-161.

[15] KACHANOV, Y.S. 1994 Physical mechanisms of laminar-boundary-layer transition. *Annu. Rev. Fluid Mech.* **26**, 411-482.

[16] LEE, S.S. 1997a Generalized critical-layer analysis of fully coupled resonant-triad interactions in boundary layers. *J. Fluid Mech.* **347**, 71-103.

[17] LEE, S.S. 1997b Generalized critical-layer analysis of instability waves in boundary layers. *Bulletin of the American Physical Society, Series II*, **42**, 2121.

[18] LEE, S.S. 1997c Spanwise periodic mean flow generated by nonlinear interaction between oblique instability waves. *Bulletin of the American Physical Society, Series II*, **42**, 2155.

[19] LEE, S. S. 1998a Nonlinear evolution of instability waves in boundary layers. *AIAA Paper*, AIAA-98-2862.

[20] LEE, S. S. 1998b Nonlinear interaction of detuned instability waves in boundary-layer transition: 2. Amplitude equations. *In preparation..*

[21] LEIB, S.J. & LEE, S.S. 1995 Nonlinear evolution of a pair of oblique instability waves in a supersonic boundary layer. *J. Fluid Mech.* **282**, 339-371.

[22] LIN, C.C. 1955 *The Theory of Hydrodynamic Stability.* Cambridge University Press.

[23] MALLIER, R. & MASLOWE, S.A. 1994 Fully coupled resonant-triad interactions in a free shear layer. *J. Fluid Mech.* **278**, 101-121.

[24] MANKBADI, R.R., WU, X. & LEE, S.S. 1993 A critical-layer analysis of the resonant triad in boundary-layer transition: nonlinear interactions. *J. Fluid Mech.* **256**, 85-106.

[25] MILES, J.W. 1962 A note on the inviscid Orr-Sommerfeld equation. *J. Fluid Mech.* **13**, 427-432.

[26] NIELD, D.A. 1972 On the inviscid solutions of the Orr-Sommerfeld equation. *Math. Chronicle* **2**, 43-52.

[27] SMITH, F.T. & BODONYI, R.J. 1982 Nonlinear critical layers and their development in streaming-flow stability. *J. Fluid Mech.* **118**, 165-185.

[28] WU, X 1992 The nonlinear evolution of high-frequency resonant-triad waves in an oscillatory Stokes layer at high Reynolds number. *J. Fluid Mech.* **245**, 553-597.

[29] Wu, X 1993 On critical-layer and diffusion-layer nonlinearity in the three-dimensional stage of boundary-layer transition. *Proc. R. Soc. Lond. A* **443**, 95-106.

[30] Wu, X 1995 Viscous effects on fully coupled resonant-triad interactions: an analytical approach. *J. Fluid Mech.* **292**, 377-407.

[31] Wu, X., Lee, S.S. & Cowley, S.J. 1993 On the weakly nonlinear three-dimensional instability of shear layers to pairs of oblique waves: the Stokes layer as a paradigm. *J. Fluid Mech.* **253**, 681-721.

[32] Wu, X., Leib, S.J. & Goldstein, M.E. 1997 On the nonlinear evolution of a pair of oblique Tollmien-Schlichting waves in boundary layers. *J. Fluid Mech.* **340**, 361-394.

[33] Wu, X., Stewart, P.A. & Cowley, S.J. 1996 On the weakly nonlinear development of Tollmien-Schlichting wavetrains in boundary layers. *J. Fluid Mech.* **323**, 133-171.

[34] Wundrow, D.W, Hultgren, L.S. & Goldstein, M.E. 1994 Interaction of oblique instability waves with a nonlinear plane wave. *J. Fluid Mech.* **264**, 343-372.

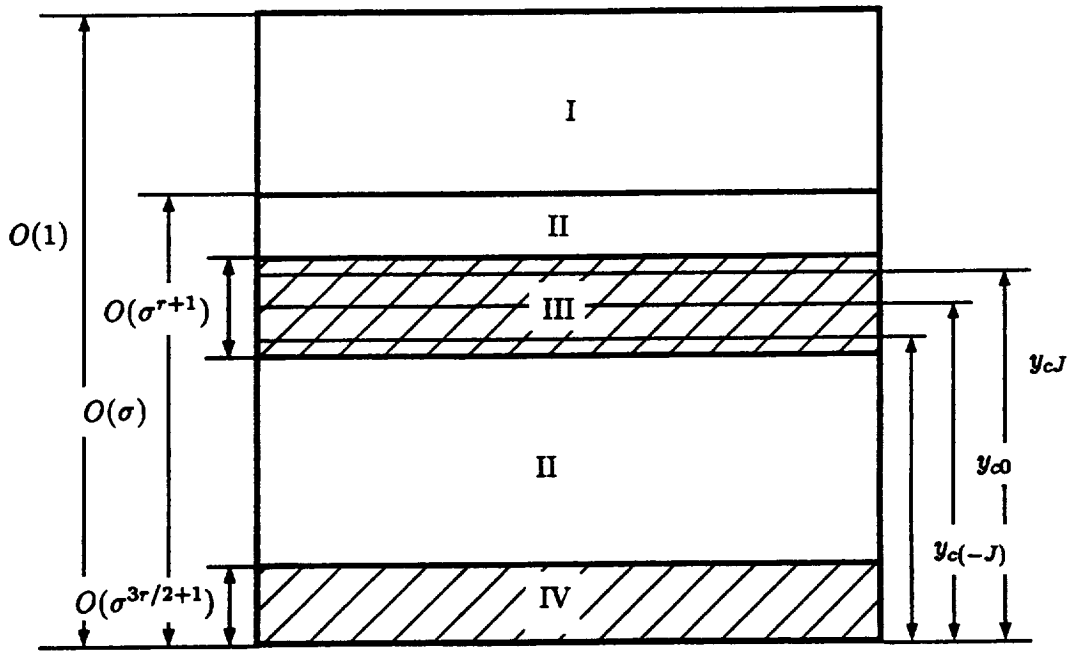

Fig. 1 Multi-layer structure for the non-equilibrium critical-layer analysis of multi-resonant-triads in boundary layers. I, main boundary layer; II, inviscid Tollmien wall layer; III, critical layer; IV, viscous Stokes layer.

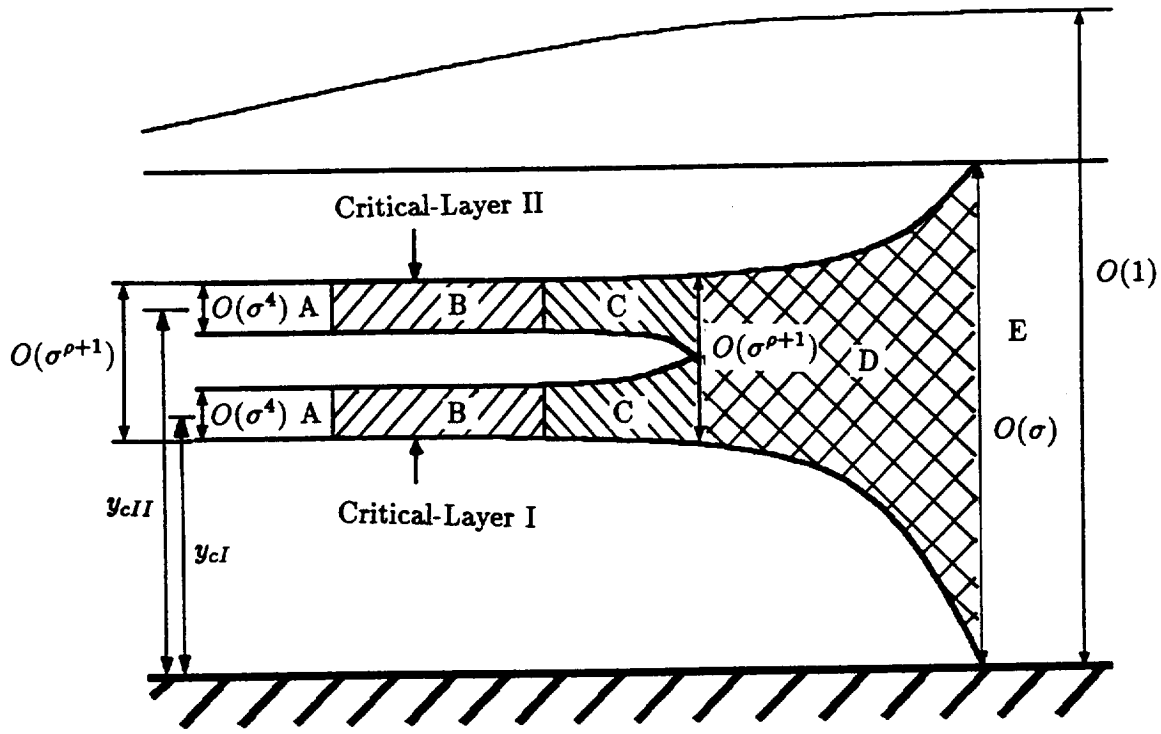

Fig. 2 Nonlinear interaction between the frequency-detuned resonant-triads I and II in an adverse-pressure-gradient boundary layer where $\rho < 3$. A, linear stage; B, parametric-resonance stage; C, fully-coupled stage; D, frequency-detuned nonlinear-interaction stage; E, triple-deck stage.

REPORT DOCUMENTATION PAGE

Form Approved
OMB No. 0704-0188

1. AGENCY USE ONLY (*Leave blank*)	2. REPORT DATE	3. REPORT TYPE AND DATES COVERED
	June 1998	Final Contractor Report

4. TITLE AND SUBTITLE

Nonlinear Interaction of Detuned Instability Waves in Boundary-Layer Transition
Resonant-Triad Interaction

5. FUNDING NUMBERS

WU–538–03–11–00
NAS3–98022

6. AUTHOR(S)

Sang Soo Lee

7. PERFORMING ORGANIZATION NAME(S) AND ADDRESS(ES)

NYMA, Inc.
2001 Aerospace Parkway
Brook Park, Ohio 44142

8. PERFORMING ORGANIZATION REPORT NUMBER

E–11230

9. SPONSORING/MONITORING AGENCY NAME(S) AND ADDRESS(ES)

National Aeronautics and Space Administration
Lewis Research Center
Cleveland, Ohio 44135–3191

10. SPONSORING/MONITORING AGENCY REPORT NUMBER

NASA CR—1998-207938

11. SUPPLEMENTARY NOTES

Project Manager, Dennis L. Huff, Structures and Acoustics Division, NASA Lewis Research Center, organization code 5940, (216) 433–3913.

12a. DISTRIBUTION/AVAILABILITY STATEMENT

Unclassified - Unlimited
Subject Category: ~~71~~ 34 Distribution: Nonstandard

This publication is available from the NASA Center for AeroSpace Information, (301) 621–0390.

12b. DISTRIBUTION CODE

13. ABSTRACT ***(Maximum 200 words)***

The non-equilibrium critical-layer analysis of a system of frequency-detuned resonant-triads is presented using the generalized scaling of Lee (1997a). It is shown that resonant-triads can interact nonlinearly within the common critical layer when their (fundamental) Strouhal numbers are different by a factor whose magnitude is of the order of the growth rate multiplied by the wavenumber of the instability wave. Since the growth rates of the instability modes become larger and the critical layers become thicker as the instability waves propagate downstream, the frequency-detuned resonant-triads that grow independently of each other in the upstream region can interact nonlinearly in the later downstream stage. In the final stage of the non-equilibrium critical-layer evolution, a wide range of instability waves with the scaled frequencies differing by almost $O(1)$ can nonlinearly interact. Low-frequency modes are also generated by the nonlinear interaction between oblique waves in the critical layer. The system of partial differential critical-layer equations along with the jump equations are presented here. The amplitude equations with their numerical solutions are given in Part 2. The nonlinearly generated low-frequency components are also investigated in Part 2.

14. SUBJECT TERMS

Nonlinear instability; Boundary layer transition; Resonant-triad

15. NUMBER OF PAGES

65

16. PRICE CODE

A04

17. SECURITY CLASSIFICATION OF REPORT	18. SECURITY CLASSIFICATION OF THIS PAGE	19. SECURITY CLASSIFICATION OF ABSTRACT	20. LIMITATION OF ABSTRACT
Unclassified	Unclassified	Unclassified	